0888-8809/07/$15.00/0
Printed in U.S.A.

Molecular Endocrinology 21(10):2440–2457

doi: 10.1210/me.2006-0402

Genetic Removal of Smad3 from Inhibin-Null Mice Attenuates Tumor Progression by Uncoupling Extracellular Mitogenic Signals from the Cell Cycle Machinery

Brendan D. Looyenga and Gary D. Hammer

Cellular and Molecular Biology Graduate Program (B.D.L., G.D.H.), and Department of Internal Medicine (G.D.H.), Division of Metabolism, Endocrinology and Diabetes, University of Michigan, Ann Arbor, Michigan 48109-2200

Inhibin and activin are members of the TGFβ family that perform mutually antagonistic signaling roles in the anterior pituitary, gonads, and adrenal gland. Unopposed activin signaling in inhibin-null (*Inha*−/−) mice causes the formation of granulosa cell tumors in the gonads and adrenal cortex, which depend upon FSH for efficient growth and progression. In this study, we demonstrate that Smad3, a key effector of activin signaling, is expressed at high levels and is constitutively activated in tumors from these mice. Removal of Smad3 from *Inha*−/− mice by a genetic cross to Smad3-null (*Madh3*−/−) mice leads to a significant decrease in cyclinD2 expression and a significant attenuation of tumor progression in the gonads and adrenal. The decrease in cyclinD2 levels in compound knockout mice is related to a reduction in mitogenic signaling through the phosphoinositide-3-kinase (PI3-kinase)/Akt pathway, which is required for normal cell cycle progression in tumor cells. Loss of PI3-kinase/Akt signaling cannot be attributed to alterations in IGF expression, suggesting instead that signaling through the FSH receptor is attenuated. Gene expression profiling in the ovaries of *Madh3*−/− and *Inha*−/−:*Madh3*−/− compound knockout mice supports this hypothesis and further suggests that Smad3 is specifically required for FSH to activate PI3-kinase/Akt, but not protein kinase A. Together these observations imply that activin/Smad3 signaling is necessary for efficient signaling by FSH in *Inha*−/− tumor cells and that interruption of this pathway uncouples FSH from its intracellular mitogenic effectors. (*Molecular Endocrinology* 21: 2440–2457, 2007)

SUCCESSFUL PRODUCTION OF mature gametes by the male and female gonads is dependent upon appropriate specification and growth of the somatic cell compartment. Somatic cells of the ovary and testis are instructively directed to differentiate and proliferate by a complex set of precisely orchestrated signals that emanate from multiple cellular sources. Although many of the early signals that direct specification of somatic cell fates are intrinsic to the local environment of the gonad, further proliferation and differentiation of these cells is dependent upon extrinsic hormonal signals from pituitary gonadotropes, which produce FSH and LH (1–3).

Studies performed in mice that have been genetically altered to lack FSH signaling have revealed that this hormone is required for proper differentiation and proliferation of ovarian granulosa cells and testicular Sertoli cells, which perform homologous functions in their respective organs (4–7). Binding of the FSH receptor (Fshr) by FSH activates a number of primary intracellular signaling pathways dependent upon adenylate cyclase, which produces the secondary messenger cAMP (8–10). Intracellular signaling mediated by cAMP has been classically understood to work through protein kinase A (PKA), although more recent studies have suggested that cAMP-mediated activation of phosphoinositide-3-kinase (PI3-kinase) and its effector Akt is equally important in FSH signal transduction (11–16). Pharmacological or genetic blockade of either PKA or PI3-kinase disrupts the ability of FSH to stimulate differentiation and proliferation in primary gonadal cell cultures, indicating the mutual importance of these two pathways for effective signaling through Fshr (15, 17).

FSH signaling to granulosa and Sertoli cells transcriptionally induces expression of the activin β-A (*Inhba*) and β-B (*Inhbb*) genes, which encode for individual subunits of the activin homodimer (18). Activins are members of the TGFβ superfamily of signaling ligands, which signal through a receptor complex composed of two type II receptors (ActRII or ActRIIB) and two type I receptors (Alk4) (19). This heterotet-

First Published Online July 24, 2007

Abbreviations: CREB, cAMP-response element binding protein; Fshr, FSH receptor; Igf1, GH/IGF-I; PCNA, proliferating cell nuclear antigen; PI3-kinase, phosphoinositide-3-kinase; PKA, protein kinase A; TBST, Tris-buffered saline/0.1% Tween 20.

***Molecular Endocrinology* is published monthly by The Endocrine Society (http://www.endo-society.org), the foremost professional society serving the endocrine community.**

rameric complex contains intrinsic serine/threonine kinase activity that directly phosphorylates and activates the secondary messenger proteins Smad2 and Smad3 (20). Upon phosphorylation, Smad2/3 proteins oligomerize with a co-Smad (Smad4) and translocate into the nucleus to mediate transcriptional events by either directly binding DNA or binding to other transcriptional complexes (21–23).

Activin signaling plays multiple roles in reproductive endocrinology, most crucially by stimulating the production of FSH in the anterior pituitary and by providing direct mitogenic signals to granulosa and Sertoli cells (24–30). Although the mechanisms by which activin mediates these functions have been extensively explored *in vitro*, the relative importance of Smad2 and Smad3 in each function has been challenging to separate because these factors transcriptionally activate both unique and overlapping sets of target genes in a cell type-specific manner (17, 31–35). Despite this difficulty, both *in vitro* and *in vivo* studies suggest that activin signaling through Smad2 is more critical for the endocrine role of activin in stimulating the production of FSH from pituitary gonadotrope cells, whereas activin signaling through Smad3 is more important for the autocrine role of activin in stimulating somatic cell differentiation and proliferation within the gonads (31, 36, 37).

The ability of activin/Smad3 to stimulate efficient cell cycle progression in somatic cells of the gonad depends upon synergistic signaling with FSH (24, 28). Specifically, FSH and activin signaling converge on the cyclinD2 (*Ccnd2*) promoter, which is transcriptionally activated by coordinate signals from PI3-kinase/Akt and Smad proteins (17). Positive expression of cyclinD2 is critical for proper growth and maturation of ovarian granulosa cells, as indicated by female cyclinD2-null (*Ccnd2*$-/-$) mice, which are infertile due to the inability of their granulosa cells to proliferate in response to FSH (38). Similar phenotypes were observed in FSHβ-null (*Fshb*$-/-$) and Smad3-null (*Madh3*$-/-$) females, strongly supporting the physiological importance of coordinate signaling by FSH and activin *in vivo* (5, 36). Although these signals do not appear to be absolutely required for male gonadal function, loss of any of them similarly compromises the Sertoli cell population and leads to decreased testicular size (29, 30).

To prevent the uncontrolled expansion of granulosa and Sertoli cells, signaling by FSH and activin must be appropriately terminated at the level of both the pituitary and the follicle. This is achieved in large part by follicular production of inhibin, an atypical TGFβ family member that functions exclusively as a competitive antagonist of other TGFβ family members (39, 40). Whereas activin is a homodimer composed of two β (Inh/Actβ) subunits, inhibin is a heterodimer composed of a unique α-subunit (Inhα) bound to one Inh/Actβ subunit (41). The heterodimeric structure of inhibin allows it to competitively inhibit activin signaling by binding only one of the two required type II receptors, thus preventing formation of the heterotetrameric receptor complex required for pathway activation (20, 42). Production of inhibin therefore effectively antagonizes follicular growth in three ways: 1) by deceasing FSH production in the pituitary; 2) by removing Actβ subunits from the pool available for homodimerization; and 3) by directly inhibiting the mitogenic signals of activin to granulosa cells.

Inhibin α-subunit knockout (*Inha*$-/-$) mice spontaneously develop gonadal tumors and—upon gonadectomy—adrenocortical tumors, both of which contain a mixed population of steroidogenic cells of gonadal identity (43–45). We have previously shown that the abnormal specification of gonadal tumor cells in the adrenal cortex of *Inha*$-/-$ mice results from chronic gonadotropin signaling, which reprograms pluripotent adrenocortical stem/progenitor cells and forces them to adopt cellular fates normally restricted to the gonad (43–45). Like the normal somatic cells of the gonad, these tumors depend upon sustained gonadotropin signaling for growth and progression and produce high levels of activin, which stimulate tumor cell growth in an autocrine fashion (44, 46, 47). Genetic crosses of *Inha*$-/-$ mice to the *Fshb*$-/-$ and *Ccnd2*$-/-$ strains lead to a significant attenuation in tumor progression, further reinforcing the similarities between hyperproliferative tumor cells and the normal somatic cells of the gonads (48, 49). Similar studies have not been carried out with *Madh3*$-/-$ mice, however, leaving unanswered the question of whether activin signaling through Smad3 plays a significant role in *Inha*$-/-$ tumorigenesis.

In this study, we have addressed the question of whether Smad3 is required for gonadal and adrenal tumorigenesis in *Inha*$-/-$ mice. Our analyses indicate that Smad3 protein is both elevated and constitutively activated in the gonadal and adrenal tumors of *Inha*$-/-$ mice, and that genetic removal of Smad3 from these animals severely attenuates tumor progression. This effect is mediated by decreases in signaling through the PI3-kinase/Akt pathway and cyclinD2 expression, indicating that Smad3 is required for efficient signaling by activin and FSH. As such, Smad3 appears to coordinate mitogenic stimuli by both of these factors and drive cell cycle progression in *Inha*$-/-$ tumor cells.

RESULTS

Smad3 Protein Is Highly Expressed and Activated in *Inha*$-/-$ Tumors

To evaluate the potential role of Smad3 in *Inha*$-/-$ tumorigenesis, we first asked whether Smad3 was present and activated in tumor cells derived from the ovary, testis, and adrenal glands. Immunoblot analysis reveals that Smad3 is expressed at very high levels in tumors from all three tissues and that it is also highly phosphorylated, presumably as a result of signaling

initiated by tumor-derived activin (Figs. 1A and 2A). The activation status of Smad3 is further reinforced by its nuclear localization in tumor cells, as revealed by immunofluorescent staining of paraformaldehyde-fixed tumor sections (Figs. 1B and 2C). The presence and activation of Smad3 in tumors supports the hypothesis that activin exerts its mitogenic effects through this protein in *Inha*−/− tumor cells.

Expression of Smad3 Accurately Identifies Tumor Progenitor Populations in the Ovary and Testis

Formation of tumors in the *Inha*−/− ovary occurs as a result of uncontrolled proliferation by granulosa cells, which are specified within the ovary during embryonic development. Immunofluorescent staining of wild-type ovaries indicates that granulosa cells strongly express Smad3 during the preantral and early antral stages of development, during which time follicles are under the control of mitogenic mechanisms mediated by FSH and activins (Fig. 1B). Mature antral and preovulatory follicles do not contain activated Smad3 protein, however, indicating that activin signaling to granulosa cells is progressively lost over the course of antral follicle maturation (Fig. 1B). Continued expression of activated Smad3 in *Inha*−/− ovarian tumors suggests that inhibin is responsible for the suppression of activin signaling during antral follicle progression. As such, the specific localization of Smad3 in the ovary accurately predicts which cell population gives rise to tumors in *Inha*−/− mice.

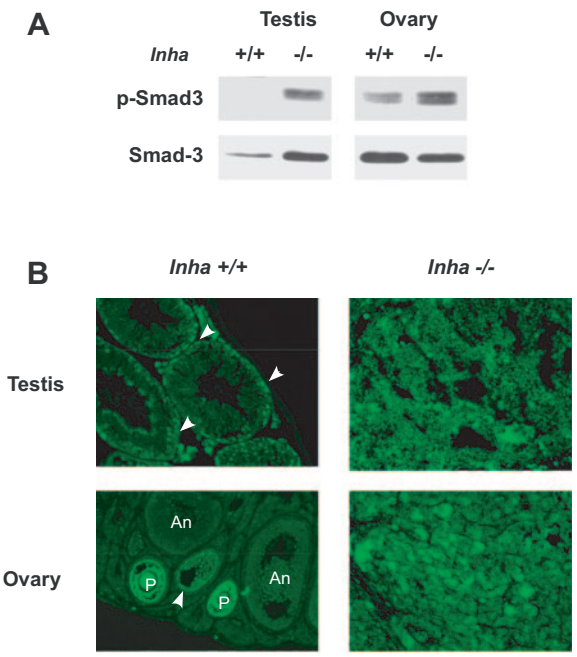

Fig. 1. Smad3 Is Expressed and Activated in the Wild-Type Ovary and *Inha*−/− Gonad Tumors, But Not in the Wild-Type Testis

A, Immunoblot analysis demonstrates that Smad3 protein is expressed and activated by phosphorylation in the wild-type ovary, but is only present at very low levels and is inactive in the testis. Both ovarian and testicular tumors from *Inha*−/− contain abundant and active Smad3 protein. B, In the wild-type ovary, Smad3 is localized to granulosa cells of preantral (P) and early antral (*arrow*) follicles. Prominent nuclear localization at the preantral stage indicates that Smad3 is activated as well. Staining for Smad3 is lost in large antral (An) follicles, indicating progressive down-regulation of activin signaling during follicular maturation. The wild-type testis displays only weak staining for Smad3 in Sertoli cells (*white arrow*). Consistent with the lack of phosphorylation, Smad3 does not appear to be nuclear localized. Tumors from both the ovary and testis contain high levels of nuclear Smad3, indicating constitutive activin signaling.

The observation that Smad3 expression correlates with the source of tumor cells in the ovary prompted us to ask whether Smad3 expression in the testis similarly correlates with the source of tumor cells. Previous studies of *Inha*−/− mice have defined a distinct pattern of events that leads to the formation of tumors within the testis and have suggested that the ultimate source of tumors in this tissue is the Sertoli cell compartment (45, 48, 49). Increased proliferation and changes in cell identity within this cellular compartment appear to precede frank tumor formation, suggesting that Sertoli cells are uniquely sensitive to loss of inhibin. Based on these observations, we predicted that Smad3 would be expressed in testicular Sertoli cells and would therefore correlate with the source of tumor cells in the testis.

Immunofluorescent staining for Smad3 in the wild-type testis reveals specific localization of Smad3 to the Sertoli cell compartment, consistent with the notion that these cells give rise to tumors in the absence of inhibin (Fig. 1B). Because Sertoli cells compose a smaller percentage of total cellular mass in the testis compared with granulosa cells in the ovary, however, the total amount of Smad3 in the testis is much less than in the ovary (Fig. 1A). Furthermore, Smad3 does not appear to be activated in the Sertoli cell compartment, as indicated by immunoblot analysis of phospho-Smad3 in the wild-type testis. Loss of inhibin within the testis apparently disturbs this homeostasis, leading to Smad3 activation and expansion of the Sertoli cell compartment. Tumor cells that derive from this expansion express high levels of activated Smad3, explaining the dramatic increase in Smad3 abundance and activation in *Inha*−/− testicular tumors compared with the wild-type testis (Fig. 1, A and B).

Expression of Smad3 Accurately Identifies Gonadotropin-Dependent Tumor Progenitor Population in the Adrenal Cortex

Gonadectomy of *Inha*−/− mice causes adrenal tumorigenesis, which is dependent upon the chronically elevated gonadotropin levels that result from this manipulation. Under these pathophysiological stimuli, we previously found that a subset of subcapsular adrenocortical cells adopt a female gonadal somatic cell

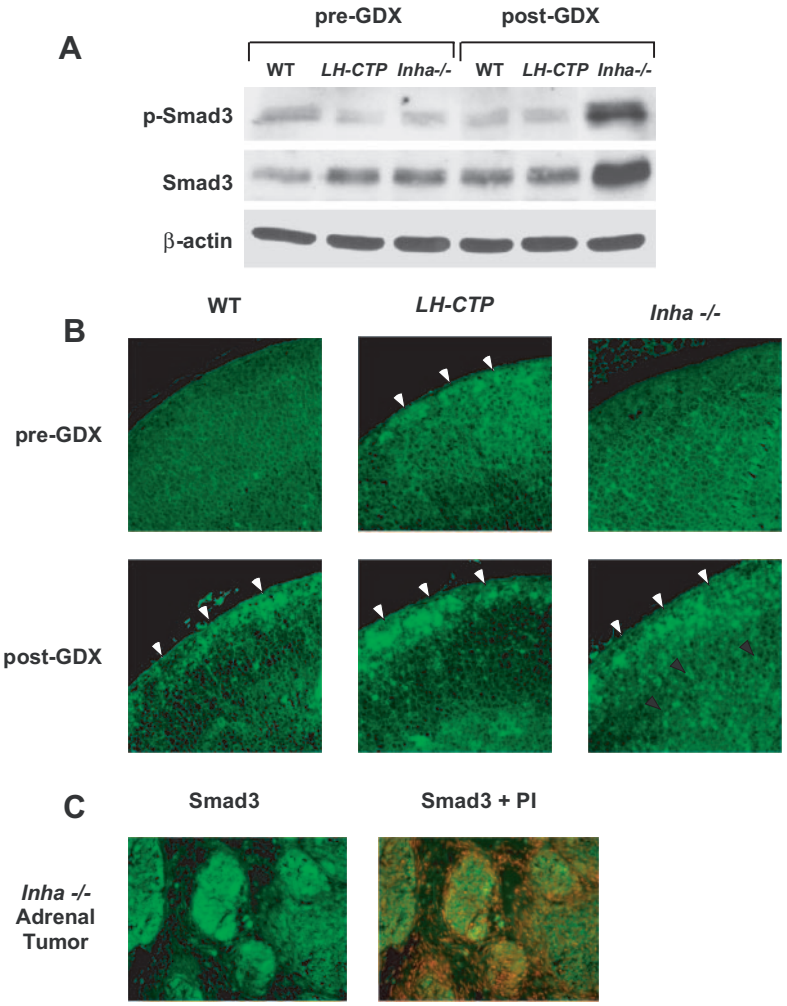

Fig. 2. Smad3 Expression and Activation in Adrenal Gland Is Stimulated by Elevated Gonadotropin Signaling

A, Immunoblot analysis demonstrates that Smad3 protein is only weakly expressed in the adrenal gland, indicating that the activin signaling pathway is not prominently involved in normal adrenal physiology. Strong expression of activated Smad3 in *Inha*−/− tumors is consistent with their phenotypic switch to a granulosa-like cellular identity. B, Both the wild-type (WT) and *Inha*−/− adrenal cortices are devoid of Smad3 staining before gonadectomy. Although immunoblotting is not sensitive enough to detect the few cells that display activated Smad3 protein after gonadectomy (GDX), immunofluorescent staining detects a small population of subcapsular cells with nuclear Smad3 in both wild-type and *Inha*−/− tissues (*white arrows*). These cells do not exist outside of the subcapsular region in wild-type mice, but persist throughout the cortex of *Inha*−/− mice (*black arrows*). A similar population of Smad3-positive cells can be detected in the subcapsular region of *bLH-βCTP* mice before and after gonadectomy, indicating that increased gonadotropin abundance is sufficient to activate activin/Smad3 signaling in subcapsular adrenocortical cells. C, Smad3-positive cells that persist in the adrenal cortex of *Inha*−/− mice give rise to adrenocortical tumors, which also show constitutively activated, nuclear Smad3. Within tumors, Smad3 expression is limited to the granulosa-like parenchymal compartment and is excluded from surrounding fibroblastic stromal cells.

identity, as seen by their ectopic expression of gonadally restricted genes such as *Gata4*, *Cyp17a1*, and *Cyp19* (43, 50). In the wild-type adrenal cortex, these cells either die or are respecified as normal adrenocortical cells, but in *Inha*−/− mice, these cells instead form tumors that are phenotypically indistinguishable from *Inha*−/− ovarian granulosa cell tumors. Because progenitor cells for *Inha*−/− tumors would be expected to express Smad3, immunostaining for this protein in the mouse adrenal permits us to test our hypothesis that *Inha*−/− adrenal tumors originate in the subcapsular stem/progenitor zone of the adrenal cortex.

Before gonadectomy, Smad3 protein is only weakly expressed in the adrenal glands of both wild-type and *Inha*−/− mice and is largely inactive based on the low level of phosphorylation in tissue lysates and lack of nuclear localization in tissue sections (Fig. 2, A and B). After gonadectomy, Smad3 phosphorylation appears to remain at basal levels in wild-type mice but is dramatically increased in tumor lysates from *Inha*−/− mice (Fig. 2A). This dramatic increase in Smad3 acti-

vation is accompanied by a similarly dramatic increase in total Smad3 protein in tumors, consistent with their known phenotypic switch to a granulosa cell identity (Fig. 2B). Interestingly, immunofluorescent detection of Smad3 protein in the adrenal cortex of wild-type mice after gonadectomy demonstrates the appearance of a small population of subcapsular cells that stain positive for accumulation of nuclear Smad3 (Fig. 2B). A similar population of cells is also found in the subcapsular region of *Inha*−/− mice after gonadectomy, although in these mice the Smad3-positive cells persist outside of the subcapsular region, suggesting that they give rise to the Smad3-positive adrenocortical tumors (Fig. 2C). Because these Smad3-positive cells appear in the adrenals of both wild-type and *Inha*−/− mice—but only persist in the *Inha*−/− mice—these data suggest that the central role of inhibin in the adrenal is to terminate signaling to Smad3, thereby blocking the ability of these cells to proliferate continuously and form tumors in the adrenal cortex.

Misspecification of adrenocortical progenitor cells toward a gonadal identity is also found in transgenic mice that produce supraphysiological levels of gonadotropins. We previously demonstrated the presence of gonadal cells in the subcapsular zone of *bLH-βCTP* mice, which display constitutively elevated levels of serum LH due to transgenic overexpression of a modified bovine LH gene (43, 51). Immunofluorescent staining for Smad3 in adrenals from *bLH-βCTP* mice shows that this population of cells is also positive for nuclear Smad3 even before gonadectomy, indicating that elevated gonadotropin levels are sufficient to activate Smad3 in the adrenal cortex (Fig. 2B). Because Smad3 is neither highly expressed nor activated in cells of the adrenal cortex under normal gonadotropin levels, these data support the assertion that the Smad3-positive cells we have identified are in fact gonadal cells that arise from pluripotent adrenocortical progenitors under the stimuli of excessive gonadotropin signaling. It would appear from these data that Smad3 activation is an obligate step in the expansion of gonadotropin-dependent adrenocortical tumors in the *Inha*−/− adrenal gland as well as in the gonads.

Genetic Removal of Smad3 from *Inha*−/− Mice Attenuates Ovarian Tumorigenesis

The constitutive activation of Smad3 in both gonadal and adrenal tumors from *Inha*−/− mice suggests a key role for activin/Smad3 signaling in the initiation and/or maintenance of these tumors. Smad3-knockout mice (*Madh3*−/−) have been previously described and are viable into adulthood, permitting a genetic cross between *Madh3*−/− mice and *Inha*−/− mice. To determine whether loss of Smad3 can rescue or attenuate *Inha*−/− gonadal tumorigenesis, we crossed *Madh3*+/− and *Inha*+/− mice and then bred males and females that were heterozygous for both genes to determine whether *Inha*−/− offspring showed differences in tumor-forming capacity or tumor size when lacking one or both alleles of Smad3. All measurements and histological analyses were performed at 2 months of age because *Inha*−/− mice invariably demonstrate large gonadal tumors at this age but do not yet develop severe health defects associated with prolonged tumor growth.

Female *Madh3*−/− mice are subfertile and show a marked increase in follicular atresia and growth arrest at the preantral stage of development (Fig. 3C) (36). This arrest in follicular development, which is caused by decreased granulosa cell proliferation and survival, is demonstrated by a 50% reduction in *Madh3*−/− ovarian weight at 2 months of age as well as by a significant decrease in the expression of cell cycle progression markers, including cyclinD2 and proliferating cell nuclear antigen (PCNA), in *Madh3*−/− ovaries (Fig. 3B). Because *Inha*−/− tumor cells appear to be under the same growth control mechanisms as normal granulosa cells and similarly express high levels of Smad3, we hypothesized that genetic removal of Smad3 would similarly attenuate *Inha*−/− tumor growth in the ovary.

By 2 months of age, *Inha*−/− ovaries on average weigh 100 times as much as the wild-type ovary (Fig. 3A). Continuously expanding clusters of tumor cells in these tissues rapidly ablate normal ovarian architecture, and as a result no intact follicles or oocytes are visible in *Inha*−/− ovarian tumors (Fig. 3C). Removal of one allele of Smad3 from *Inha*−/− mice causes a roughly 50% reduction in tumor mass, whereas removal of both alleles almost completely attenuates tumor growth (Fig. 3A). Histological examination of *Inha*−/−:*Madh3*−/− ovaries shows the retention of several oocytes surrounded by small follicles, although follicular development is arrested in a similar fashion to *Madh3*−/− ovaries (Fig. 3C). At the periphery of the ovary, a mass of expansive stromal tissue indicates that tumorigenesis still occurs in the absence of Smad3, albeit at a much slower rate than when Smad3 is present.

Genetic Removal of Smad3 from *Inha*−/− Mice Attenuates Testicular Tumorigenesis

Madh3−/− male mice are fertile and have testes that are similar in histological appearance to wild-type testes. Due to a decrease in somatic cell numbers during development, however, *Madh3*−/− testes are slightly smaller than wild-type tissues as indicated by their decrease in seminiferous tubule diameter (Fig. 4C). *Inha*−/− males also initially demonstrate normal testicular architecture and begin to produce sperm but rapidly develop Sertoli/granulosa cell tumors that on average weigh three to five times that of the normal testis by 2 months of age (Fig. 4A). Removal of one allele of Smad3 has no statistical effect on testicular tumor weight, whereas removal of both alleles results in a significant decrease in testicular weight, suggestive of tumor rescue (Fig. 4A).

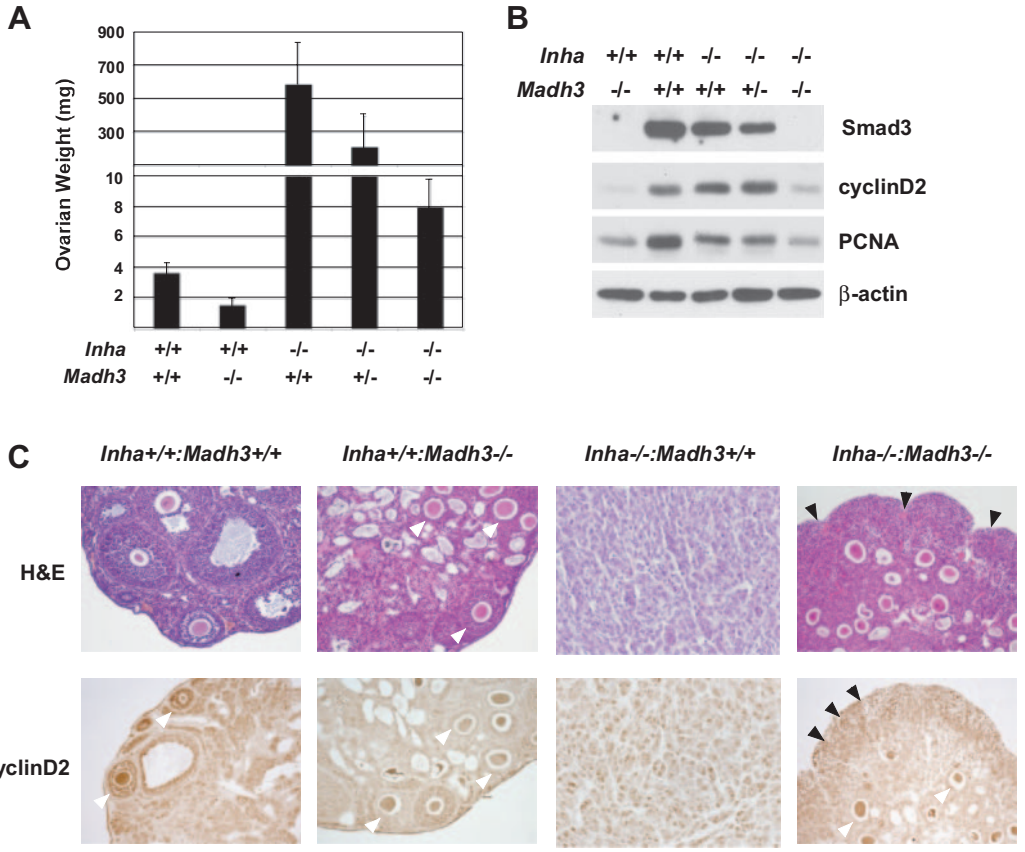

Fig. 3. Removal of Smad3 from *Inha*−/− Mice Attenuates Ovarian Tumor Progression and Reduces Cellular Expression of CyclinD2

Mice heterozygous for both *Inha* and *Madh3* were mated, and ovarian weight of their female offspring was measured at 2 months of age. A, *Madh3*−/− ovaries are smaller than wild-type ovaries due a reduction in granulosa cell mass. *Inha*−/− mice produce massive ovarian tumors by 2 months, which on average weigh over 500 mg. Removal of one allele of *Smad3* (*Inha*−/−:*Madh3*+/−) reduced tumor size by half, whereas removal of both alleles (*Inha*−/−:*Madh3*−/−) almost completely rescues ovarian weight. B, Immunoblot analysis of ovarian lysates demonstrates that tissue weight correlates with the abundance of Smad3 and the expression of cell cycle progression markers cyclinD2 and PCNA. C, Ovaries from *Madh3*−/− mice display an increase in atretic follicles and small preantral follicles (*white arrows*), few of which progress to the antral stage. Immunohistochemical analysis demonstrates that cyclinD2 is considerably lower in *Madh3*−/− follicles compared with follicles of similar size in the wild-type ovary. Tumors from *Inha*−/− mice display a complete loss of normal ovarian structure and are composed of clusters of granulosa cells that express abundant cyclinD2. Tissue architecture is partially rescued in *Inha*−/−:*Madh3*−/− ovaries, although most of the follicles are small or atretic like those seen in *Madh3*−/− ovaries (*white arrows*). *Inha*−/−:*Madh3*−/− ovaries frequently contain proliferating tumor tissue near the periphery (*black arrows*) that stain positive for cyclinD2, indicating that while tumor progression is delayed, tumor initiation is not completely rescued.

Histological analysis of testicular tumors in *Inha*−/− mice indicates the presence of large, hemorrhagic tumors that lie adjacent to remnants of seminiferous tubules (Fig. 4C). Signs of spermatogenesis within the tubules are usually absent due to the expansion of Sertoli cells into the lumen of the tubule, which leads to loss of germ cells and normal tubule architecture. The increased cellularity of these tumors is visible in the tight compaction of granulosa cell clusters and is reflected by the increase in β-actin content that tumors contain relative to the normal testis (Fig. 4B).

In contrast to the *Inha*−/− testes, testes from compound knockout males at 2 months of age show very few histological defects, although they do display larger seminiferous tubules than *Madh3*−/− mice and contain small regions of focal Sertoli cell hyperplasia, which are associated with early stages of tumor formation (Fig. 4C). We did not detect any frank tumors in the testes of compound mutant mice by histological analysis at 2 months of age; however, the appearance of Sertoli lesions suggests that tumor progression in *Inha*−/− mice is delayed by loss of Smad3 and is not completely rescued.

Genetic Removal of Smad3 from *Inha*−/− Mice Attenuates Adrenal Tumorigenesis

We next asked whether removal of Smad3 from *Inha*−/− mice would also rescue adrenal tumorigenesis, as would be predicted based on the known phe-

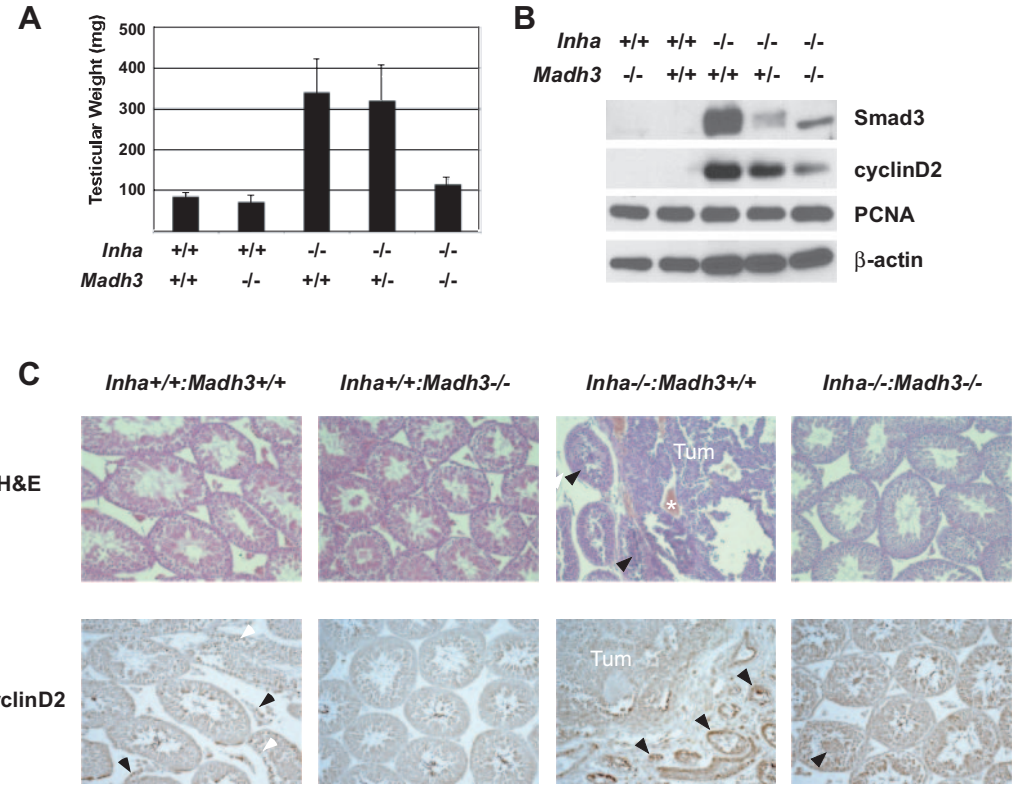

Fig. 4. Removal of Smad3 from *Inha*−/− Mice Delays Testicular Tumor Formation and Reduces Expression of CyclinD2

Mice heterozygous for both *Inh* and *Smad3* were mated, and testicular weight of their male offspring was measured at 2 months of age. A, *Madh3*−/− mice show a slight reduction in testicular weight consistent with their overall decrease in body size. *Inha*−/− display a 3- to 4-fold increase in testicular weight due to formation of large tumors, whereas *Inha*−/−:*Madh3*−/− mice display a near complete rescue of testicular weight. No effect was observed by removal of only one allele of Smad3 from *Inha*−/− mice. B, Testicular tumors from *Inha*−/− mice express dramatically higher levels of Smad3 than wild-type mice, and demonstrate an increase in cellularity reflected by the increase in β-actin levels. Tumors also express high levels of cyclinD2, which decrease moderately with removal of Smad3. Expression of the generic proliferative marker PCNA is uninformative in testicular lysates, because testicular germ cells demonstrate a high mitotic index during spermatogenesis that masks any changes in somatic cell proliferation. Note that the lower band in the Smad3 panel corresponds to cross-reactive staining for Smad2, which continues to be expressed in Smad3-deficient tumors. C, Removal of Smad3 from the testis has little effect on testicular architecture or function, although seminiferous tubules in *Madh3*−/− mice are smaller than those in wild-type mice. Neither wild-type nor *Madh3*−/− testis contain significant amounts of cyclinD2, although it is weakly present in Sertoli (*white arrows*) and Leydig cells (*black arrows*) in the wild-type testis. Testicular tumors from *Inha*−/− mice appear as dense masses of small, proliferating cells that express abundant cyclinD2. These tumors arise from hyperproliferative Sertoli cells, which occlude the lumen of seminiferous tubules (*black arrow*) and similarly stain positive for cyclinD2. Gross testicular architecture and spermatogenesis are rescued in *Inha*−/−:*Madh3*−/−, although small masses of focal Sertoli cell hyperplasia (*black arrow*) are detected with a few of the tubules. Cells within the tubules also demonstrate staining for cyclinD2, indicating the presence of premaligant lesions—but not frank tumors—in compound knockout mice.

notypic similarities between ovarian and adrenal tumors in these mice. To answer this question, we gonadectomized compound knockout mice at 5 wk of age and permitted them to progress to end-stage disease, characterized by overall cachexia, which is indicative of the formation of large adrenal tumors. Only female mice were used for this study because gonadectomized female *Inha*−/− mice develop adrenocortical tumors more rapidly than their male counterparts and respond more favorably to surgical manipulation in our experience.

Although the initiation of adrenocortical tumorigenesis in *Inha*−/− mice is highly stochastic after gonadectomy, these mice proceed to end-stage disease along a relatively predictable time course that can be quantified as survival time to end-stage disease. Although *Inha*−/− mice display a 50% survival rate of 22 wk after gonadectomy (n = 7), removal of only one allele of Smad3 from this genetic background (n = 8) results in a 50% survival rate of 37.5 wk (Fig. 5A). All mice in this study developed large adrenocortical tumors at the time of death, indicating that extensive adrenal tumor burden was the likely cause of mortality. Tumors from both sets of mice display typical histology, characterized by masses of small, highly proliferative granulosa-like cells infiltrated with fibroblastic stromal tissue.

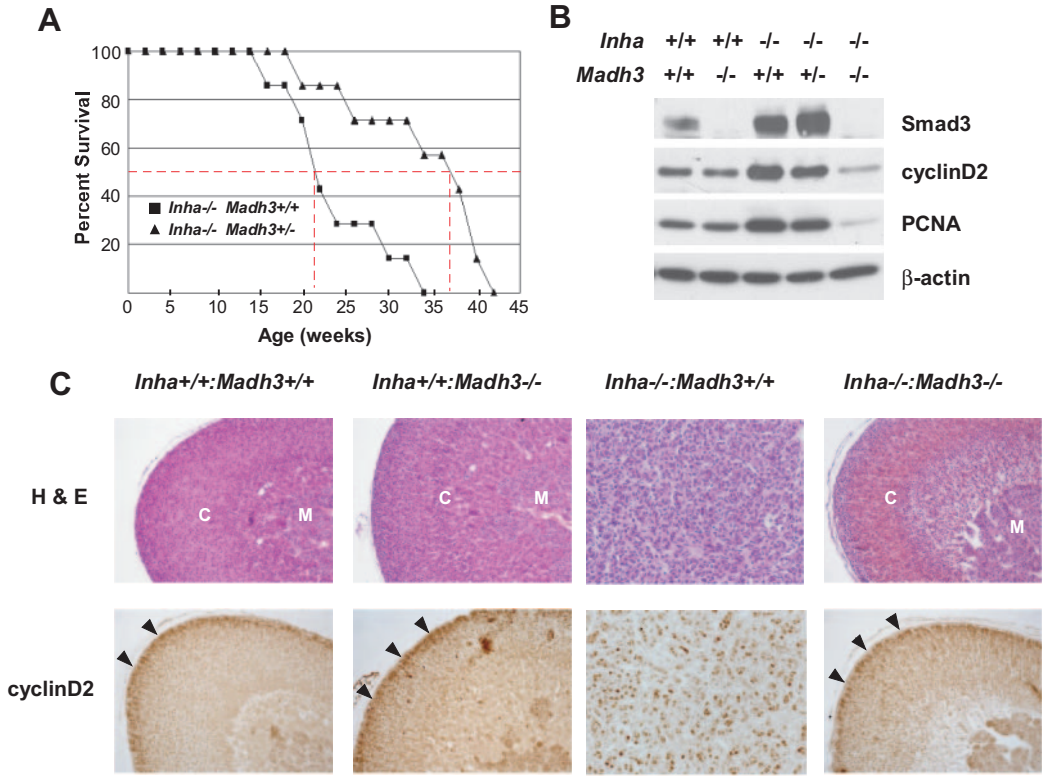

Fig. 5. Removal of Smad3 from *Inha*−/− Mice Attenuates Adrenal Tumor Progression and Reduces Cellular Expression of CyclinD2

Mice heterozygous for both *Inh* and *Smad3* were mated, and their offspring were gonadectomized at 5 wk of age. Gonadectomized mice were allowed to proceed to end-stage adrenal disease before euthanasia. A, Percent survival over a 45-wk time course is displayed for *Inha*−/−*:Madh3*+/+ (n = 7) and *Inha*−/−*:Madh3*+/− (n = 8) mice. All mice displayed advanced adrenal tumors at time of death. Removal of one allele of Smad3 delays progression to end-stage disease by an average of 10.5 wk, increasing survival time in these mice by 57%. The effect of removing both alleles of Smad3 could not be quantified due to the poor postoperative survival of *Madh3*−/− mice, although of the mice that did survive surgical manipulation (3 of 10), none had developed adrenal tumors at the time of death up to 30 wk after gonadectomy. B, Wild-type and *Madh3*−/− mice display no differences in expression of the cell cycle markers cyclinD2 and PCNA. Tumors from *Inha*−/− mice express higher levels of both cell cycle markers, consistent with the increased rate of proliferation. Expression of both markers is reduced by removal of Smad3 in a dose-dependent fashion. C, *Madh3*−/− mice display normal adrenal histology characterized by appropriate zonation of the cortex (C) and position relative to the adrenal medulla (M). CyclinD2 expression in these tissues is enriched in the subcapsular zone (*black arrows*) and is not effected by the absence of Smad3 in *Madh3*−/− mice. *Inha*−/− mice develop dense adrenocortical tumors that are histologically similar to those seen in the ovary and display strong immunohistochemical staining for cyclinD2. Adrenals from *Inha*−/−*:Madh3*−/− mice do not show any evidence of tumorigenesis under histological analysis and retain normal adrenal structure as long as 32 wk after gonadectomy. CyclinD2 expression in these tissues is localized to the subcapsular region and similar in intensity to that seen in wild-type animals.

Unfortunately, we were unable to quantify the effect of removing both alleles of Smad3 from *Inha*−/− mice due to the poor long-term survival of *Madh3*−/−, which had been previously described in inbred and mixed genetic backgrounds (52). In addition, these mice were refractive to surgical manipulation and survived gonadectomy surgery very poorly. Of the mice that did survive gonadectomy (3 of 10 females), none had developed adrenocortical tumors by the time of death at 20 or more weeks after gonadectomy. Furthermore, all three mice demonstrated normal adrenal architecture upon histological examination (Fig. 5C). The cause of death in one of these mice appeared to be the development of colorectal tumors, which has been previously described in *Madh3*−/− mice, whereas the cause of death in the other two mice could not be determined (52). Despite this shortcoming, the attenuation in tumor progression seen in *Inha*−/−*:Madh3*+/− mice still suggests that Smad3 is required for efficient adrenal tumor progression.

CyclinD2 Expression Is Down-Regulated by Removal of Smad3 from *Inha*−/− Mice

The significant delay in tumor progression that we observed when Smad3 is removed from *Inha*−/− mice suggests that ovarian, testicular, and adrenal tumor cells—like normal granulosa cells—progress through the cell cycle less rapidly in the absence of mitogenic signaling through Smad3. Previous studies have indi-

cated that Smad3 participates in the transcriptional activation of cyclinD2, a specific regulator of the G_1/S phase of the cell cycle that is required for proliferation of granulosa cells (17, 38). Genetic removal of cyclinD2 from mice produces a similar phenotype to *Madh3*−/− mice and also attenuates tumor progression in the *Inha*−/− strain (48). Based on these previous observations, we hypothesized that loss of Smad3 attenuates tumorigenesis in *Inha*−/− mice by decreasing cyclinD2 levels.

To test this hypothesis, we analyzed the expression of cyclinD2 and the nonspecific proliferative marker PCNA in the ovaries, testes, and adrenals from mice of all genotypes from our study. Both immunoblots and immunohistochemical staining in *Madh3*−/− ovaries reveal that expression of cyclinD2 is specifically lost in the granulosa cell compartment of preantral follicles, which correlates with their decreased proliferation and frequent arrest at the preantral stage of development (Fig. 3, B and C). In contrast, follicles from wild-type mice display strong staining for cyclinD2 in the granulosa cell compartment and demonstrate active proliferation as assessed by high levels of PCNA expression (Fig. 3B).

As expected based on their granulosa cell identity, *Inha*−/− ovarian tumors exhibit robust expression of cyclinD2, which is visible as a punctate nuclear stain by immunohistochemical analysis of tumor sections (Fig. 3, B and C). Genetic removal of Smad3 from *Inha*−/− mice leads a significant reduction in ovarian cyclinD2 levels, which parallels the dramatic loss of PCNA expression in compound knockout ovaries (Fig. 3B). These data suggest that attenuation of ovarian tumor cell growth in the absence of Smad3 is mediated at least in part by decreased expression of cyclinD2, which delays tumor cell progression through the cell cycle (Fig. 3B).

Within the wild-type adult testis, cyclinD2 is very weakly expressed in both the Sertoli and Leydig cell compartments (Fig. 4, B and C). Abundant PCNA expression is still detected, however, due to the rapid proliferation of germ cells within the seminiferous tubules. Nearly identical results are obtained in adult *Madh3*−/− testes, which display little change in overall cellular proliferation or cyclinD2 expression (Fig. 4B). These findings suggest that neither Smad3 nor cyclinD2 is required for normal reproductive function in the adult testis and that instead their expression and/or activation are specifically suppressed in the wild-type testis to prevent abnormal Sertoli cell proliferation.

In contrast to wild-type and *Madh3*−/− testes, *Inha*−/− testicular tumors exhibit strong expression of cyclinD2, which directly correlates with their dramatic elevation of Smad3 protein levels (Fig. 4, B and C). Interestingly, these changes also occur in the Sertoli cell compartment before tumor formation, suggesting that unopposed activin signaling to Sertoli cells directly induces their hyperproliferation and subsequent formation of tumors (Fig. 4C). Removal of Smad3 from these tissues moderately decreases cyclinD2 levels, supporting a link between Smad3 and cyclinD2 transcription.

In the wild-type adrenal gland, cyclinD2 is expressed at moderate levels and primarily localizes to the subcapsular zone of the cortex (Fig. 5, B and C). Expression of cyclinD2 in the normal adrenal does not appear to be controlled by Smad3 signaling, however, because *Madh3*−/− mice show no change in adrenal cyclinD2 levels (Fig. 5B). Ectopic expression of Smad3 in *Inha*−/− adrenocortical tumors results in a significant up-regulation in cyclinD2 levels and overall proliferation, again suggesting a direct link between activin/Smad3 signaling and cyclinD2 expression. Genetic removal of Smad3 from *Inha*−/− adrenal tumors has a similar effect to that observed in gonadal tumors, resulting in significant reduction in cyclinD2 and a decrease in proliferation (Fig. 5B). These data together imply that tumor cells in *Inha*−/− mice—regardless of their tissue of origin—rely upon the same Smad3-dependent signaling mechanism to drive cyclinD2 expression, and that this mechanism is necessary for cell cycle progression and tumor growth.

Smad3 Deficiency Causes Partial Insensitivity to FSH in the Ovary and in *Inha*−/− Ovarian Tumors

The mechanistic relationship between Smad3 and cyclinD2 expression is likely to involve both direct binding of activated Smad3 to the cyclinD2 promoter and indirect modulation of signaling by gonadotropins, particularly FSH. The latter assertion is based on previous studies that showed *Madh3*−/− granulosa cells are resistant to FSH signaling, although they express normal levels of Fshr in the ovary and produce elevated levels of FSH from the anterior pituitary (36). We similarly found that Fshr was expressed at levels comparable to wild-type ovaries in *Madh3*−/− ovaries and in the ovaries of *Inha*−/−*:Madh3*−/− compound knockout mice, suggesting that defects in FSH sensitivity likely lie downstream of Fshr (Fig. 6A).

Despite having normal or elevated levels of FSH and Fshr, *Madh3*−/− mice and *Inha*−/−*:Madh3*−/− mice both show defects in FSH-induced gene expression. Several genes that are absent from *Fshb*−/− mice, including *Lhr*, *Cyp11a1*, and *Cdkn1b*, are similarly repressed in the absence of Smad3, suggesting that Smad3 is required for efficient FSH signaling (Fig. 6, B and C) (18). Interestingly, however, another set of genes that is normally absent from *Fshb*−/− mice, including *Inhba* and *Sgk*, are expressed at or near normal levels in *Madh3*−/− mice and *Inha*−/−*:Madh3*−/− mice, indicating that signaling through Fshr is only selectively repressed.

Smad3 Deficiency Selectively Attenuates FSH Signaling through the PI3-Kinase/Akt Pathway

Because multiple effector pathways lie downstream of Fshr, we hypothesized that the selective repression of

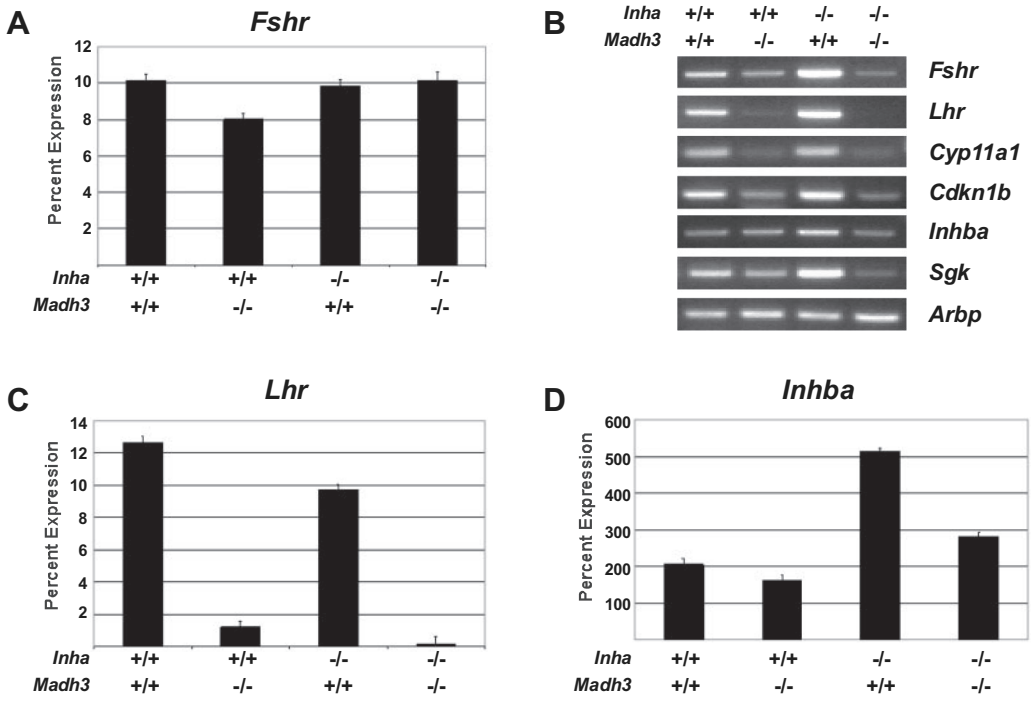

Fig. 6. Smad3-Deficient Ovaries Are Partially Insensitive to FSH

A, Quantitative RT-PCR detection of *Fshr* transcripts in ovaries from 5-wk-old wild-type, *Madh3−/−*, *Inha−/−* and *Inha−/−:Madh3−/−* compound knockout mice demonstrates that *Fshr* is expressed at or near normal levels in the absence of Smad3. B, RT-PCR detection of FSH-induced genes in ovaries from 5-wk-old wild-type, *Madh3−/−*, *Inha−/−* and *Inha−/−:Madh3−/−* compound knockout mice demonstrates that mice deficient in Smad3 are unable to activate transcription of several genes including *Lhr*, *Cyp11a1*, and *Cdkn1b*. Other genes that are absent in FSH-deficient (*Fshb−/−*) mice, including *Inhba* and *Sgk*, are expressed, indicating that Smad3 deficiency causes only a partial loss of sensitivity to FSH in the ovary. C and D, Quantitative RT-PCR analysis of *Lhr* and *Inhba* transcripts reinforces the different expression pattern of these two genes in the absence of Smad3. Although expression of *Lhr* is severely compromised by loss of Smad3, *Inhba* is expressed at or near normal levels. Expression of both of these genes in granulosa cells depends upon FSH signaling, suggesting that loss of Smad3 only partially affects the ability of FSH to induce transcription through Fshr signaling.

specific FSH target genes in *Madh3−/−* and *Inha−/−:Madh3−/−* mice may result from the specific loss of signaling through only one of these pathways. As noted above, the two most prominent intracellular effectors of FSH signaling are the PKA and PI3-kinase/Akt pathways, both of which depend upon FSH-induced cAMP production (9, 15). Consistent with a decrease in FSH sensitivity, we found that *Madh3−/−* ovaries display reduced activation of the PI3-kinase/Akt signaling cascade, indicated by a decrease in Akt and Foxo1 phosphorylation (Fig. 7A). Foxo1 functions as a transcriptional repressor on the cyclinD2 (*Ccnd2*) promoter and is normally removed from the nucleus by FSH signaling through PI3-kinase/Akt to facilitate transcription of the *Ccnd2* gene in granulosa cells (17). Down-regulation of PI3-kinase/Akt activity indicates that cyclinD2 levels may in part be repressed due to the inability of *Madh3−/−* cells to efficiently clear Foxo1 from the *Ccnd2* promoter.

To assess the activity of PKA in wild-type and *Madh3−/−* ovaries, we analyzed the phosphorylation status of cAMP-response element binding protein (CREB), which is directly activated by PKA in response to increased intracellular levels of cAMP. Interestingly, signaling through PKA appears not to be disrupted by loss of Smad3, as indicated by similar levels of CREB phosphorylation in wild-type and *Madh3−/−* ovaries (Fig. 7A). These data suggest that Smad3 is specifically required for stabilization of FSH signaling to the PI3-kinase pathway but is not required to maintain FSH signaling to PKA.

Removal of Smad3 from *Inha−/−* ovarian tumors has a similar effect on FSH effector pathways to that seen in *Madh3−/−* granulosa cells. *Inha−/−:Madh3−/−* compound knockout ovaries display a significant reduction in Akt and Foxo1 activation, whereas the total expression of these molecules is unchanged (Fig. 7A). Although total CREB levels are decreased by removal of Smad3 from *Inha−/−* ovarian tumors, the ratio of phospho-CREB:CREB remains relatively constant, suggesting that PKA activation is not affected by loss of Smad3.

We also measured the effect of Smad3 removal on PI3-kinase/Akt and PKA signaling in the testis and adrenals. *Madh3−/−* mice display no differences in either pathway compared with wild-type mice in these tissues, supporting our previous assertion that Smad3 does not play a prominent role in testicular or adrenal

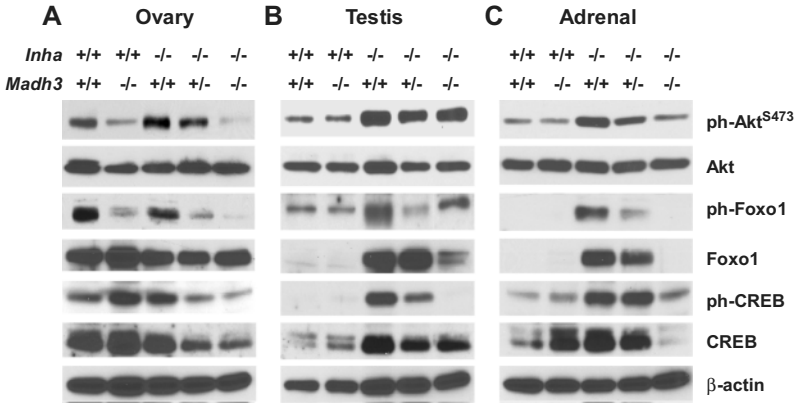

Fig. 7. Signaling through the PI3-Kinase/Akt Pathway Is Selectively Attenuated by Removal of Smad3 from the Ovary and *Inha*−/− Tumors

Expression and activation of FSH signaling pathways was measured by immunoblot analysis in the ovaries, testes, and adrenals of wild-type, *Madh3*−/−, *Inha*−/−, and *Inha*−/−*:Madh3*−/− compound knockout mice. A, In the ovary, removal of Smad3 selectively down-regulates signaling through the PI3-kinase/Akt pathway, but has no effect on PKA signaling as assessed by the phosphorylation of the PKA effector CREB. As a result of decreased Akt activation, Foxo1 is not phosphorylated in *Madh3*−/− granulosa cells. Removal of Smad3 from *Inha*−/− ovarian tumors also attenuates Akt and Foxo1 activation, but has no effect on the overall expression of these molecules. Although total CREB levels are decreased by removal of Smad3 from tumors, the ratio of phospho-CREB:CREB remains relatively constant, suggesting that PKA activation is not affected by loss of Smad3. B and C, Removal of Smad3 from the testis (B) and adrenal (C) has no effect on basal levels of signaling through the PI3-kinase/Akt and PKA/CREB pathways, which are generally activated at lower levels compared with the ovary. Neither of these tissues express appreciable amounts of Foxo1, which appears to be restricted to granulosa cells in the ovary. Testes and adrenals from *Inha*−/− mice contain abundant Foxo1, however, indicating the presence of tumors with a primarily granulosa cell identity. These tumors also demonstrate significant elevations in the expression and activation of components of the PI3-kinase/Akt and PKA/CREB signaling pathways, consistent with their dependence upon FSH signaling for growth and progression. Removal of Smad3 from the testes and adrenals of *Inha*−/− mice causes a significant decrease in Akt activation, although it has no effect on the total level of Akt expression. Decreased activation of Akt parallels decreased tumor burden in the testis and adrenal, which is evident from the loss of Foxo1 and CREB expression in *Inha*−/−*:Madh3*−/− compound mutant tissues.

physiology (Fig. 7, B and C). Interestingly, neither of these tissues express appreciable amounts of Foxo1, which is a specific marker of granulosa cells within the various steroidogenic lineages of the gonads and adrenal (53, 54). Formation of granulosa cell tumors in *Inha*−/− testes and adrenals is clearly indicated by their expression of Foxo1, as well as elevated expression and activation of components of the PI3-kinase/Akt and PKA/CREB signaling pathways (Fig. 7, B and C). These data are consistent with the assertion that all *Inha*−/− tumors are primarily composed of granulosa cells, which depend upon FSH signaling for growth and tumor progression.

Removal of Smad3 from the testes and adrenals of *Inha*−/− mice causes a significant decrease in Akt activation, although it has no effect on the total level of Akt expression. Although immunoblot analysis appears to indicate that CREB phosphorylation is similarly repressed by removal of Smad3 from *Inha*−/− testicular and adrenal tumors, measurements of total CREB protein instead demonstrate that CREB phosphorylation decreases with Smad3 removal because total levels of CREB protein are decreased. Rather than indicating a specific effect on PKA signaling, these data instead suggest that decreased phospho-CREB staining in *Inha*−/−*:Madh3*−/− tumors represents a decrease in tumor burden in the testis and adrenal compared with normal tissue, which is also present in tissue lysates from these animals. This assertion is supported by coincident loss of Foxo1 expression in *Inha*−/−*:Madh3*−/− testes and adrenals, which—as noted above—marks the presence of granulosa tumor cells within these tissues. Together, these data are consistent with our hypothesis that Smad3 deficiency selectively attenuates FSH signaling to PI3-kinase/Akt but has no effect on FSH signaling to PKA, in normal granulosa cells and in *Inha*−/− tumor cells.

Smad3 Deficiency Decreases Systemic Igf1 Levels, But Not Intraovarian Igf1 Levels

The observation that *Madh3*−/− mice exhibit a defect in somatic growth that reduces their body weight by 30% compared with wild-type littermates suggests a defect in the GH/IGF-I (Igf1) axis, which regulates somatic growth in mice and other vertebrate species (52, 55, 56). This growth defect is similar to that seen in activin A-deficient (*Inhba*−/−) mice, which have been previously shown to exhibit low levels of systemic Igf1 (55). Measurements of serum Igf1 levels by RIA confirm this hypothesis, indicating that both *Madh3*−/− mice and *Inha*−/−*:Madh3*−/− compound mutant mice have 35–45% lower levels of systemic Igf1 than wild-type or *Inha*−/− mice (Fig. 8A). These data are

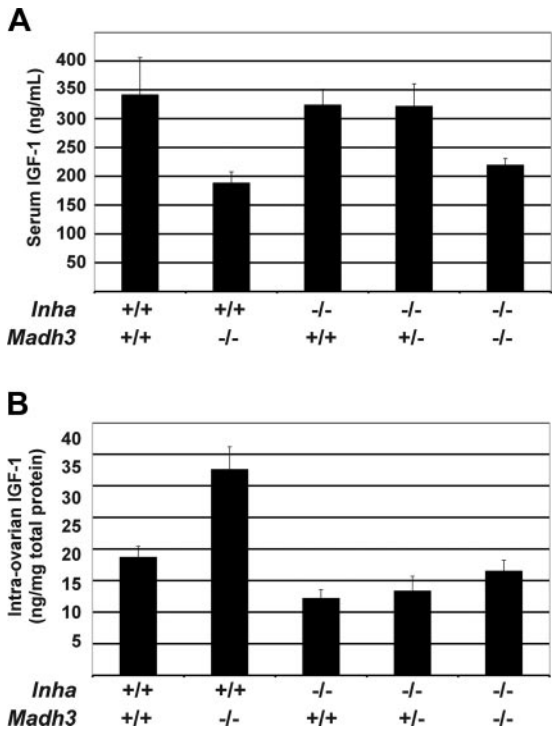

Fig. 8. Smad3 Deficiency Reduces Circulating Igf1 Levels But Does Not Decrease Intraovarian Igf1 Production

Serum and ovarian tissue were collected from the 5-wk-old offspring of mice heterozygous for both *Inh* and *Smad3*. Serum and tissue content of Igf1 were measured by RIA. A, *Madh3*−/− mice display a 35–40% reduction in circulating Igf1, whereas changes in *Inh* genotype had no effect on serum Igf1 levels. Reduction of Igf1 in *Madh3*−/− mice correlates with a roughly 30% decrease in total body weight. B, *Madh3*−/− ovaries display an increase in relative intraovarian Igf1 (Igf1/total protein) compared with wild-type ovaries, which probably reflects the relative increase in the number of growth-arrested preantral follicles. *Inha*−/− ovarian tumors actually have decreased relative Igf1 content compared with wild-type (*Inh*+/+*:Smad3*+/+) ovaries, suggesting that the Igf1 signaling pathway is not prominently activated in tumors. Removal of Smad3 from *Inha*−/− mice has almost no effect on tumor production of Igf1, indicating that modulation of Igf1 signaling is not likely to play a role in the rescue affected by this genetic cross.

consistent with the hypothesis that Smad3 is required for efficient production of Igf1 by hepatocytes in response to activin-A signaling.

Intrafollicular production of Igf1 is important for growth of immature granulosa cells in primary and secondary follicles (3, 57, 58). Signaling of Igf1 through its receptor (Igf1r) activates PI3-kinase/Akt signaling, suggesting that this ligand may be responsible for activation of the cyclinD2 promoter in granulosa cells before their dependence upon FSH signaling. As such it is possible that decreased autocrine production of Igf1 could contribute to the attenuation of PI3-kinase/Akt signaling and tumor growth in *Inha*−/−*:Madh3*−/− compound mutant tissues independent of any relationship between Smad3 and FSH.

To test whether removal of Smad3 from the ovary resulted in decreased intrafollicular Igf1 production, we performed RIA measurements of total Igf1 protein in ovarian protein lysates. Interestingly, relative intraovarian Igf1 levels (Igf1/total protein) were decreased 35% in *Inha*−/− mice but were increased 70% in *Madh3*−/− mice compared with wild-type littermates (Fig. 8B). Intraovarian Igf1 levels did not vary significantly between *Inha*−/−*:Madh3*−/− and wild-type littermates, indicating that Smad3 does not regulate the expression of Igf1 within the ovary. RIA measurements were confirmed using a sandwich ELISA for Igf1, which showed a similar trend among the different genotypes examined (data not shown). As such, these data suggest that changes in Igf1 signaling are unlikely to play any significant role in the attenuation of tumorigenesis observed in *Inha*−/−*:Madh3*−/− mice. Because the assays indicated above measure total Igf1 and do not distinguish between free ligand and that bound to IGF-binding proteins, however, it is impossible to exclude potential differences in Igf1 bioactivity based on differential interactions with serum binding proteins.

DISCUSSION

Inhibin knockout mice provide a unique model of endocrine tumorigenesis that is fully penetrant across both sexes in both the gonads and adrenals. Although tumors derived from these different tissues demonstrate a large amount of histopathological variability, it is also clear that they share a number of common features including the expression of similar genes and the synthesis of estrogen as a primary steroid product (43, 45, 50). Together, these findings suggest that at least one of the key cellular identities within all *Inha*−/− tumors is that of differentiated granulosa cells. Results from this study are consistent with this assertion, indicating that cellular mechanisms that control granulosa cell proliferation are conserved in *Inha*−/− tumors, regardless of their tissue of origin.

In this study, we show that the activin effector protein Smad3 is highly stabilized and activated in all *Inha*−/− tumors, identical to what is observed in proliferating granulosa cells of preantral follicles. Interestingly, expression of Smad3 characterizes all of the individual cell types that give rise to *Inha*−/− tumors in the ovary, testis, and adrenal, suggesting that its uncontrolled activation is an early step in tumor formation. To determine whether signaling through Smad3 is required for tumorigenesis, we crossed Smad3-null (*Madh3*−/−) mice to *Inha*−/− mice and performed analysis of tumor progression and animal survival at specific timepoints. Data from these *in vivo* studies indicate that loss of Smad3 significantly attenuates the rate of tumor growth in *Inha*−/− mice, although it does not prevent the abnormal specification of the granulosa cell identity in the testis and adrenal. As such, it

appears that Smad3 plays a critical role in *Inha*−/− tumor progression, but not in the initiation of tumor formation in the gonads and adrenal.

Because *Madh3*−/− mice exhibit a significant reduction in somatic growth, we questioned whether the effect on tumor growth that we observed in *Inha*−/−:*Madh3*−/− mice might be a result of reduced intraovarian Igf1 rather than a specific effect on FSH signaling. Previous studies on activin-A-deficient mice (*Inhaa*−/−) demonstrated that activin is necessary for normal somatic growth, and that loss of activin-A results in reduced levels of serum Igf1 (55). We found that *Madh3*−/− mice exhibit a similar reduction in circulating Igf1, indicating that Smad3 is the primary mediator of activin-induced Igf production in heptocytes. This is apparently not true within ovarian granulosa cells, however, because *Madh3*−/− and *Inha*−/−:*Madh3*−/− mice demonstrate normal or elevated levels of intraovarian Igf1 compared with wild-type littermates. It is unlikely that reduced serum levels of Igf1 have any significant effect on granulosa cell proliferation and follicular growth because mice with tissue-specific removal of Igf1 from the liver (LID mice) have reduced circulating Igf1 but display normal fertility (59). As such, these data imply that the effect of Smad3 removal on the PI3-kinase/Akt pathway in ovarian granulosa cells is specifically related to a decrease in FSH sensitivity as opposed to a loss of Igf1 signaling.

We propose that loss of Smad3 attenuates *Inha*−/− tumorigenesis by uncoupling extracellular mitogenic signals from the cell cycle machinery, in particular cyclinD2 (Fig. 9). Attenuation of cyclinD2 expression is likely due to the direct absence of Smad3 on the cyclinD2 (*Ccnd2*) promoter, as well as the general insensitivity of Smad3-null tumor cells to FSH signaling (17, 36). The latter effect appears to be an indirect consequence of removing Smad3 and is revealed by severe down-regulation of signaling through the PI3-kinase/Akt pathway. This critical mitogenic pathway impacts cyclinD2 expression by removing the transcriptional repressor Foxo1 from the *Ccnd2* promoter, thereby allowing for positive transactivation by factors such as Smad3 (17). Together, these effects lead to severe attenuation of cyclinD2 expression and inefficient progression of tumor cells through the G_1/S phase of the cell cycle (38).

The centrality of cyclinD2 expression to *Inha*−/− tumor cell proliferation is supported by a previous genetic cross between *Ccnd2*−/− mice and *Inha*−/− mice, which demonstrate attenuated tumor progression very similar in nature to what we observed in our study. *Ccnd2*−/−:*Inha*−/− mice exhibit increased survival over time and smaller tumors at a fixed timepoint, although loss of cyclinD2 does not completely rescue tumorigenesis (48). Interestingly, *Inha*−/− animals heterozygous for *Ccnd2* (*Inha*−/−:*Ccnd2*+/−) display an intermediate degree of tumor attenuation, which we also observed in our model. The remarkable similarity between these models therefore suggests that the critical role of activin signaling through Smad3 is to facilitate cell cycle progression by activation of cyclinD2 expression. Signaling of activin through Smad2 ostensibly accounts for its remaining mitogenic effects, which likely explain the incomplete rescue we observed in *Inha*−/−:*Madh3*−/− mice.

The critical importance of FSH signaling to cyclinD2 expression is also reinforced by mouse modeling, in this case by a genetic cross between FSHβ-subunit knockouts (*Fshb*−/−) and *Inha*−/− mice. Mice from this study essentially phenocopy *Inha*−/−:*Madh3*−/− mice and *Inha*−/−:*Ccnd2*−/− mice, demonstrating a marked attenuation of tumor progression, but not complete rescue (49). These studies and ours clearly indicate that efficient activation of cyclinD2—and therefore efficient proliferation of tumor cells—absolutely depends upon cooperative mitogenic signaling by FSH to PI3-kinase/Akt and activin to Smad3. These pathways, however, do not operate in isolation, but are critically linked together such that loss of one pathway inevitably compromises the other.

Because expression of the activin-β subunit genes (*Inhba* and *Inhbb*) requires FSH signaling in granulosa/tumor cells, it is obvious that Smad3 activation in these cells is linked to FSH signaling by its control of activin ligand availability (18). The converse relationship is less clear, however, although it has been convincingly proven that *Madh3*−/− mice are functionally insensitive to FSH signaling (36). Regulation of FSH signaling by Smad3 is at the level of neither the ligand nor the receptor, however, because levels of both FSH and Fshr have been reported to be normal or elevated in *Madh3*−/− mice (36).

A recent study of the ovarian phenotype in *Madh3*−/− mice demonstrated that FSH insensitivity is incomplete at the transcriptional level because a few known target genes of FSH are still expressed, including the activin β-subunit genes (36). Because these genes are almost completely absent from the ovary in *Fshb*−/− mice, this study implies that the dependence of FSH signaling on Smad3 may be pathway-specific (18). Results from our study strongly support these previous findings and show further that transcriptional regulation of several FSH-induced genes is retained in *Inha*−/−:*Madh3*−/− tumors, despite their delayed progression and loss of cyclinD2 expression. Immunoblot analysis of *Madh3*−/− ovaries and *Inha*−/−:*Madh3*−/− tumors reveals that differences in gene expression between mice that lack FSH and mice that lack Smad3 may be a result of the selective disruption of FSH signaling to PI3-kinase/Akt in the absence of Smad3, which does not impinge upon the ability of FSH to signal to PKA. As such, any FSH target genes that are induced solely by PKA/CREB—such as the *Inhba* gene—are normally expressed in Smad3-deficient tissues, whereas those that depend upon Akt signaling are significantly down-regulated. Together, these data suggest that crosstalk between the activin and FSH signaling pathways specifically

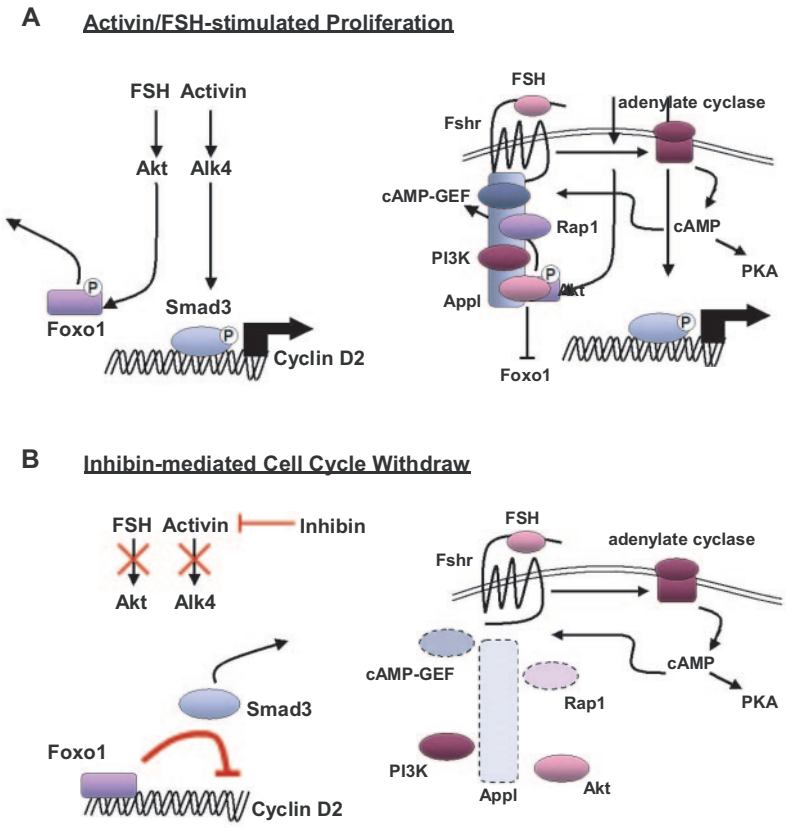

Fig. 9. A Hypothetical Model for Akt Activation by FSH and Activin in Granulosa Cells and in *Inha*−/− Granulosa Cell Tumors

A, Proliferation of antral granulosa cells is primarily controlled by FSH, which activates the activin/Smad3 signaling pathway by transcriptionally up-regulating activin subunit expression. Previous studies indicate that FSH and activin signaling converge on the cyclinD2 promoter, which is coordinately regulated by Foxo1 and Smad proteins. Activin signaling through Smad2 and Smad3 transcriptionally activates cyclinD2, whereas FSH signaling through Akt removes the negative regulator Foxo1 from the cyclinD2 promoter (17). Activation of Akt by FSH in granulosa cells depends upon cAMP, which is generated by adenylate cyclase in response to heterotrimeric G protein signaling by Fshr. Although cAMP activates PKA, this pathway is not required for activation of Akt. A composite model generated by several previous studies (see *Discussion*) suggests instead that cAMP activates Akt via a complex of proteins that may be physically tethered to Fshr via the adaptor protein Appl. This complex likely includes cAMP-dependent guanine-nucleotide exchange factors, which activate members of the Rap1 family of small G proteins. Rap1 family proteins subsequently recruit and activate the p110 and p85 subunits of PI3-kinase (PI3K), which is responsible for activation of Akt. B, In the presence of inhibin—or the absence of Smad3—positive regulation of the cyclinD2 promoter is lost, whereas negative regulation by Foxo1 is maintained. The relationship between activin/Smad3 signaling and FSH/Akt signaling is unclear at this time, but likely involves regulation at the level of the signaling complex that physically links Fshr to PI3-kinase and Akt. In the absence of signaling through Smad3, formation of this complex may be disrupted by the lack of one or more critical components needed to couple Fshr to PI3-kinase/Akt. We have not detected a change in the absolute levels of Akt in *Madh3*−/− ovaries, suggesting that some other component of the complex is missing and that Fshr is therefore unable to appropriately recruit or activate Akt. Because Smad3 is known only to function as a transcriptional regulator, it is likely that one or more components of the complex are under the direct transcriptional control of activin/Smad3 signaling. As such, inhibin is able to interrupt FSH signaling to granulosa cells by down-regulating the activin/Smad3 pathway, which effectively uncouples Fshr from PI3-kinase/Akt and causes cell cycle withdrawal of these cells in the late antral follicle due to the down-regulation of mitogenic effectors, including cyclinD2.

occurs at the level of PI3-kinase/Akt, and not at the level of Fshr or adenylate cyclase.

A more detailed understanding of how activin/Smad3 signaling impinges upon cellular sensitivity to FSH will require a better understanding of the mechanism that FSH uses to stimulate PI3-kinase/Akt, which has only been partially elucidated at this time. Multiple studies suggest that the well-described up-regulation of cAMP by Fshr is required to activate PI3-kinase/Akt, but that this mechanism is independent of PKA (14, 15). The connection between cAMP and PI3-kinase/Akt may instead be mediated through cAMP-regulated guanine nucleotide exchange factors and the small GTPase Rap1, which are known to activate PI3-kinase activity (60–63). Physical interaction of these proteins with Fshr might be facilitated by the adaptor protein containing PH domain, PTB domain, and Leucine zipper motif (Appl), which was recently

identified as a Fshr binding partner by a yeast-two-hybrid approach (64). Because Appl has also been shown to bind Akt, the p110 subunit of PI3-kinase and small GTPase proteins, it could conceivably act as a scaffold for the enzymatic machinery required for Fshr to activate Akt (Fig. 9A) (65, 66). The presence of all of these components in a single complex with Fshr has yet to be demonstrated, however, indicating the need for further investigation.

Because Smad3 has not been shown to have any molecular functions outside of its ability to transcribe genes, it seems likely that its role in facilitating efficient FSH signal transduction depends upon its transcriptional induction of one or more components of the complex needed to link Fshr to the PI3-kinase/Akt pathway. In the absence of Smad3, these components would also be lacking, and FSH would become uncoupled from the PI3-kinase/Akt pathway (Fig. 9B). As such, simple inhibition of Smad3 is sufficient to interrupt a significant component of both the activin and FSH signaling pathways. This model is particularly attractive because it explains how and why inhibin is sufficient to prevent uncontrolled granulosa cell proliferation in the antral follicle and why its absence results in the unabated induction of cyclinD2 through both the FSH and activin signaling pathways.

MATERIALS AND METHODS

Experimental Animal Treatment and Care

All experiments involving animals were performed in accordance with institutionally approved and current animal care guidelines from University of Michigan Committee on Use and Care of Animals. Generation and genotyping of mice with a targeted deletion of the α-inhibin gene (*Inha*$-/-$), targeted deletion of the Smad3 gene (*Madh3*$-/-$), and mice harboring the *bLH-βCTP* transgene under control of the bovine LH α-subunit promoter have been described previously (45, 51, 52). The initial cross between *Inha*$-/-$ and *Madh3*$-/-$ mice resulted in mixed C57/BL6 and 129S1 genetic background. Because survival of *Madh3*$-/-$ mice is improved on mixed genetic backgrounds, we chose to maintain the C57/BL6 $\times$ 129S1 mixed background for the duration of the study (52).

For the gonadal tumor studies, all measurements and histological analyses were performed at 2 months of age because *Inha*$-/-$ mice invariably demonstrate large gonadal tumors at this age but do not yet develop severe health defects associated with prolonged tumor growth. For each group of mice analyzed in these studies, a number of five or greater was used to perform tissue weight analysis, which is presented as a mean tissue weight with error bars representing SD values.

For the adrenal tumor studies, surgical gonadectomies were performed at the age of 5 wk, and mice were euthanized at 15 wk or more after gonadectomy at the indication of end-stage disease, characterized by severe weight loss, hunched posture, and sunken eyes. Choosing a fixed timepoint at which to euthanize mice in this study was not feasible because the initiation of adrenal tumorigenesis in *Inha*$-/-$ mice is variable. A significant difficulty with this approach is the poor postoperative survival of *Madh3*$-/-$ mice, which perhaps results from the wound-healing or immunological defects that these mice display. No male mice (0 of 10) from the *Inha*$-/-$*:Madh3*$-/-$ genotype survived more than 5 d after gonadectomy, and only three female mice (3 of 10) survived longer than 20 wk after gonadectomy, at which point *Inha*$-/-$ mice invariably exhibit large adrenocortical tumors. *Madh3*$-/-$ mice also develop colorectal tumors later in life, which accounted for the death of two of the female mice that did survive past 20 wk after gonadectomy. As such we chose to analyze only female mice in this study and were unable to quantify long-term survival to end-stage adrenocortical disease.

Tissue Histology: Hematoxylin and Eosin Staining

Ovaries, testis, and adrenals were collected at indicated ages and fixed for 2–3 h in 4% paraformaldehyde/PBS. Tissues were dehydrated in graded ethanols and methyl salicylate and embedded in paraffin before sectioning. Sections were cut at 6-μm thickness and floated on prewarmed and wetted glass slides to remove any surface inconsistencies in the sections. Water was removed from under the sections by gentle aspiration, and the sections were dried overnight at 37 C to promote adherence to the slides. After drying, sections were deparaffinized in xylenes and rehydrated in graded ethanols followed by deionized water. Sections were stained for 5 sec in hematoxylin solution (Sigma, St. Louis, MO), washed in deionized water, and stained for 3 sec in eosin solution (Sigma). The sections were then washed and dehydrated in graded ethanols and xylenes, then mounted and coverslipped with Permount solution (Sigma).

Tissue Histology: Immunofluorescent Staining

Ovaries and adrenals were collected at indicated ages and prepared for histological staining as above, except that final rehydration steps were performed in Tris-buffered saline/0.1% Tween-20 (TBST, pH 7.5), in addition to deionized water. Antigen retrieval was performed by boiling rehydrated sections in 1 mM EDTA or 10 mM sodium citrate for 15 min, followed by one wash in deionized water and two washes in TBST at room temperature. Tissue sections were then blocked in antibody diluent solution (TBST, 5% BSA, 0.1% Tween-2 containing 5% normal goat serum) for 1 h, and then incubated with anti-Smad3 (1:100; Zymed Laboratories, South San Francisco, CA) or anti-phospho-Akt^{473} (1:200, immunohistochemistry-specific antibody; Cell Signaling Technology, Boston, MA) overnight at 4 C in a hydration chamber. The next day, sections were washed three times for 5 min in TBST, and then exposed to biotinylated secondary antibodies for 30 min at room temperature. After three wash steps, sections were incubated with streptavidin-FITC for 30 min at room temperature to fluorescently label stained tissue. Sections were finally washed three times more with TBST, nuclear co-stained with 4, 6-diamino-2-phenylindole or propidium iodide, and coverslipped with aqueous mounting media (Biomeda, Foster City, CA). Fluorescent images were captured with an RT-Slider digital camera and Spot (version 4.6) software (both from Diagnostic Instruments, Sterling Heights, MI).

Immunoblotting

Ovaries, testis, and adrenals were removed, dissected from surrounding adipose and connective tissue, and immediately snap frozen in liquid nitrogen. Protein lysates were collected by briefly sonicating frozen tissues in lysis buffer (40 mM HEPES, 120 mM sodium chloride, 10 mM sodium pyrophosphate, 10 mM sodium glycerophosphate, 1 mM EDTA, 50 mM sodium fluoride, 0.5 mM sodium orthovanadate, 1% Triton X-100) containing protease inhibitor cocktail (Sigma), followed by 1-h rotation at 4 C to solubilize proteins. Soluble protein was collected from centrifuged total lysates and quantified by Bradford assay. SDS-PAGE was performed on

Table 1. Primer Sequences for Semiquantitative and Quantitative RT-PCR Analysis

Gene/Transcript Name	Abbreviation	Sense Primer	Antisense Primer	Annealing Temperature (C)
FSH receptor	*Fshr*	AAG GTC TAT TCC CTG CCC AAC CAT	CTG GGT TCA TCA TCT ACG AGA GAG	57
LH receptor	*Lhr*	CTG CTG TGC TTT CAG GAA TTT GCC	ACC CTA AGG AAG GCA TAG CCC ATA	60
$P450_{scc}$	*Cyp11a1*	CTG CTT CAC CAC CCT GAG A	AGC TGC ATT CGG TTC CTG T	59
$p27^{Kip1}$	*Cdkn1b*	GTG CCT TTA ATT GGG TCT CAG GCA	AAT CTT CTG CAG CAG GTC GCT T	60
Inhibin/activin-bA	*Inhba*	GAG ATC GTA GAG GCT GTC AAG	CAC TTC TGC ACG CTC CAC TAC	57
Serum/glucocorticoid-regulated kinase	*Sgk*	CTC AAC AAA TCA ACC TGG GTC CGT	TAC TTC TTC TGC CTT GTG CCT AGC	60
Acidic ribosomal phosphoprotein	*Arbp*	CGT GAT GCC CAG GGA AGA	TCC CAC AAT GAA GCA TTT TGG	60

9–10% polyacrylamide Tris-glycine gels loaded with 10–40 μg of protein per sample, and separated proteins were transferred to nitrocellulose membranes using a semidry transfer unit. After transfer, membranes were blocked 1 h in 4% nonfat dry milk in TBST, and then incubated overnight at 4 C with primary rabbit antibodies against phospho-Smad3 (1:1000), Smad3 (1:1000; Zymed), phospho-Akt^{473} (1:1000; Cell Signaling), total Akt (1:1000; Cell Signaling), phospho-Foxo1 (1:1000; Cell Signaling), total Foxo1 (1:1000; Santa Cruz Biotechnology, Santa Cruz, CA), cyclinD2 (1:1000; Santa Cruz, M-20), PCNA (1:1000; Santa Cruz), $P450_{aromatase}$ (1:1000; Abcam, Cambridge, MA), phospho-CREB (1:500; Upstate Biotechnology, Waltham, MA), or CREB (1:1000; Upstate), or primary mouse antibodies against β-actin (1:5000; Sigma). The next day, membranes were washed three times for 5–10 min in TBST, and then incubated with horseradish peroxidase-labeled goat antirabbit or antimouse secondary antibody for 1 h at room temperature. After three more washes in TBST, membranes were incubated for 2–5 min in West Dura ECL reagent (Pierce, Rockford, IL), and then exposed to film for detection.

RT-PCR and Real-Time PCR

Tissues were removed, cleaned, and snap frozen as above. Frozen tissues were lysed in Trizol reagent using an electric tissue homogenizer, and total RNA was collected according to the manufacturer's recommended protocol. In the case of cultured cells, the total cell pellet was washed once with PBS, and then directly harvested in Trizol reagent with vigorous pipetting to homogenize the cellular lysates. Total RNA was treated with DNase (Ambion) to remove any residual genomic DNA, and was quantified by UV spectrometry. One microgram of total RNA was used to synthesize cDNA using the *iScript* kit (Bio-Rad, Hercules, CA) according to the manufacturer's recommended protocol. The final cDNA product was purified and eluted in 50 μl of Tris-EDTA buffer using PCR purification columns (QIAGEN, Hilden, Germany). One microliter of this product was used as template for all subsequent semiquantitative PCRs. Primer sequences and thermocycling conditions for each gene are shown in Table 1. Amplified products were resolved on 1–2% agarose gels and detected with ethidium bromide staining on a UV lamp.

For quantitative, real-time PCR analysis of mRNA transcript abundance, PCRs were made up using a 2× SYBR Green PCR mastermix (Applied Biosystems, Foster City, CA) along with gene-specific primers, and thermocycling was performed in the *ABI 7300* thermocycler system (Applied Biosystems). Each quantitative measurement was normalized to Rox dye as an internal standard and performed in triplicate. Transcript abundance was normalized to the average C_t value of mouse acidic ribosomal phosphoprotein (*Arbp*) for each sample. For mRNA quantitation directly from adrenal or tumor tissue, measurements were performed with a number (n) of four or greater, with n being the number of individual tissue samples from different animals.

Igf1 Protein Quantification

Age-matched experimental animals were sedated with isofluorane and decapitated, and blood was collected from each animal in an EDTA-coated capillary vial. The vials were placed on ice before separation of sera from blood cells by centrifugation at 6000 rpm for 10 min at 4 C. Purified serum was frozen at −80 C until analysis by RIA. Ovaries from the same mice were removed, dissected from surrounding adipose and connective tissue, and immediately snap-frozen in liquid nitrogen. Protein lysates from the frozen tissue were collected in the same way as performed for immunoblotting. Igf1 protein was quantified using a RIA kit specific for mouse Igf1 (Diagnostic Systems, Webster, TX). Both sera and ovary lysates were acid-extracted according to the manufacturer's instructions before measurement. All values were calculated relative to known concentrations of mouse Igf1 standard. For ovarian protein quantification, all values were normalized to the total protein input to produce a relative intraovarian Igf1 value. A number of five or greater was used for each genotype analyzed in these experiments. Error bars for the data presented above were calculated as SD values from the mean value.

Acknowledgments

The *Inha*−/− strain of mice was generated and provided by Dr. Martin Matzuk (Baylor College of Medicine, Houston, TX), whereas the *bLH-βCTP* mice were generated and provided by Dr. John Nilson (Washington State University, Pullman, WA). *Madh3*−/− mice originally generated in the laboratory of Dr. Luis Parrada (University of Texas Southwestern, Dallas, TX) were obtained from Jackson Laboratory (Bar Harbor, ME). The phospho-Smad3 antibody was provided by Dr. Michael Reiss (Cancer Institute of New Jersey, New Brunswick, NJ).

Received September 25, 2006. Accepted July 16, 2007.

Address all correspondence and requests for reprints to: Gary D. Hammer, M.D., Ph.D., BSRB 1502, 109 Zina Pitcher Place, Ann Arbor, Michigan 48109-2200. E-mail: ghammer@umich.edu.

Disclosure Statement: The authors have nothing to disclose.

REFERENCES

1. Kumar TR 2005 What have we learned about gonadotropin function from gonadotropin subunit and receptor knockout mice? Reproduction 130:293–302
2. McNatty KP, Moore LG, Hudson NL, Quirke LD, Lawrence SB, Reader K, Hanrahan JP, Smith P, Groome NP,

Laitinen M, Ritvos O, Juengel JL 2004 The oocyte and its role in regulating ovulation rate: a new paradigm in reproductive biology. Reproduction 128:379–386
3. Richards JS, Russell DL, Ochsner S, Hsieh M, Doyle KH, Falender AE, Lo YK, Sharma SC 2002 Novel signaling pathways that control ovarian follicular development, ovulation, and luteinization. Recent Prog Horm Res 57: 195–220
4. Dierich A, Sairam MR, Monaco L, Fimia GM, Gansmuller A, LeMeur M, Sassone-Corsi P 1998 Impairing follicle-stimulating hormone (FSH) signaling in vivo: targeted disruption of the FSH receptor leads to aberrant gametogenesis and hormonal imbalance. Proc Natl Acad Sci USA 95:13612–13617
5. Kumar TR, Wang Y, Lu N, Matzuk MM 1997 Follicle stimulating hormone is required for ovarian follicle maturation but not male fertility. Nat Genet 15:201–204
6. Lei ZM, Mishra S, Zou W, Xu B, Foltz M, Li X, Rao CV 2001 Targeted disruption of luteinizing hormone/human chorionic gonadotropin receptor gene. Mol Endocrinol 15:184–200
7. Ma X, Dong Y, Matzuk MM, Kumar TR 2004 Targeted disruption of luteinizing hormone β-subunit leads to hypogonadism, defects in gonadal steroidogenesis, and infertility. Proc Natl Acad Sci USA 101:17294–17299
8. Dias JA, Cohen BD, Lindau-Shepard B, Nechamen CA, Peterson AJ, Schmidt A 2002 Molecular, structural, and cellular biology of follitropin and follitropin receptor. Vitam Horm 64:249–322
9. Fontaine YA, Fontaine-Bertrand E, Salmon C, Delerue-Lebelle N 1971 [Stimulation in vitro by the 2 hypophyseal gonadotropic hormones (LH and FSH) of the adenylcyclasic activity of the ovary in the prepuberal female rat]. C R Acad Sci Hebd Seances Acad Sci D 272:1137–1140
10. Grasso P, Reichert Jr LE 1989 Follicle stimulating hormone (FSH) induces G protein dissociation from FSH receptor-G protein complexes in reconstituted proteoliposomes. Biochem Biophys Res Commun 162: 1214–1221
11. Conti M 2002 Specificity of the cyclic adenosine 3′,5′-monophosphate signal in granulosa cell function. Biol Reprod 67:1653–1661
12. Ratoosh SL, Richards JS 1985 Regulation of the content and phosphorylation of RII by adenosine 3′,5′-monophosphate, follicle-stimulating hormone, and estradiol in cultured granulosa cells. Endocrinology 117:917–927
13. Richards JS, Haddox M, Tash JS, Walter U, Lohmann S 1984 Adenosine 3′,5′-monophosphate-dependent protein kinase and granulosa cell responsiveness to gonadotropins. Endocrinology 114:2190–2198
14. Alam H, Maizels ET, Park Y, Ghaey S, Feiger ZJ, Chandel NS, Hunzicker-Dunn M 2004 Follicle-stimulating hormone activation of hypoxia-inducible factor-1 by the phosphatidylinositol 3-kinase/AKT/Ras homolog enriched in brain (Rheb)/mammalian target of rapamycin (mTOR) pathway is necessary for induction of select protein markers of follicular differentiation. J Biol Chem 279:19431–19440
15. Gonzalez-Robayna IJ, Falender AE, Ochsner S, Firestone GL, Richards JS 2000 Follicle-stimulating hormone (FSH) stimulates phosphorylation and activation of protein kinase B (PKB/Akt) and serum and glucocorticoid-induced kinase (Sgk): evidence for a kinase-independent signaling by FSH in granulosa cells. Mol Endocrinol 14: 1283–1300
16. Zeleznik AJ, Saxena D, Little-Ihrig L 2003 Protein kinase B is obligatory for follicle-stimulating hormone-induced granulosa cell differentiation. Endocrinology 144: 3985–3994
17. Park Y, Maizels ET, Feiger ZJ, Alam H, Peters CA, Woodruff TK, Unterman TG, Lee EJ, Jameson JL, Hunzicker-Dunn M 2005 Induction of cyclin D2 in rat granulosa cells requires FSH-dependent relief from FOXO1 repression coupled with positive signals from Smad. J Biol Chem 280:9135–9148
18. Burns KH, Yan C, Kumar TR, Matzuk MM 2001 Analysis of ovarian gene expression in follicle-stimulating hormone β knockout mice. Endocrinology 142:2742–2751
19. Harrison CA, Gray PC, Koerber SC, Fischer W, Vale W 2003 Identification of a functional binding site for activin on the type I receptor ALK4. J Biol Chem 278: 21129–21135
20. Lebrun JJ, Vale WW 1997 Activin and inhibin have antagonistic effects on ligand-dependent heteromerization of the type I and type II activin receptors and human erythroid differentiation. Mol Cell Biol 17:1682–1691
21. Attisano L, Wrana JL, Cheifetz S, Massague J 1992 Novel activin receptors: distinct genes and alternative mRNA splicing generate a repertoire of serine/threonine kinase receptors. Cell 68:97–108
22. Mathews LS 1994 Activin receptors and cellular signaling by the receptor serine kinase family. Endocr Rev 15: 310–325
23. Mathews LS, Vale WW 1993 Molecular and functional characterization of activin receptors. Receptor 3:173–181
24. Miro F, Hillier SG 1996 Modulation of granulosa cell deoxyribonucleic acid synthesis and differentiation by activin. Endocrinology 137:464–468
25. Woodruff TK, Lyon RJ, Hansen SE, Rice GC, Mather JP 1990 Inhibin and activin locally regulate rat ovarian folliculogenesis. Endocrinology 127:3196–3205
26. Gregory SJ, Kaiser UB 2004 Regulation of gonadotropins by inhibin and activin. Semin Reprod Med 22:253–267
27. Bilezikjian LM, Blount AL, Donaldson CJ, Vale WW 2006 Pituitary actions of ligands of the TGF-β family: activins and inhibins. Reproduction 132:207–215
28. El-Hefnawy T, Zeleznik AJ 2001 Synergism between FSH and activin in the regulation of proliferating cell nuclear antigen (PCNA) and cyclin D2 expression in rat granulosa cells. Endocrinology 142:4357–4362
29. Coerver KA, Woodruff TK, Finegold MJ, Mather J, Bradley A, Matzuk MM 1996 Activin signaling through activin receptor type II causes the cachexia-like symptoms in inhibin-deficient mice. Mol Endocrinol 10:534–543
30. Kumar TR, Varani S, Wreford NG, Telfer NM, de Kretser DM, Matzuk MM 2001 Male reproductive phenotypes in double mutant mice lacking both FSHβ and activin receptor IIA. Endocrinology 142:3512–3518
31. Bernard DJ 2004 Both SMAD2 and SMAD3 mediate activin-stimulated expression of the follicle-stimulating hormone β-subunit in mouse gonadotrope cells. Mol Endocrinol 18:606–623
32. Lamba P, Santos MM, Philips DP, Bernard DJ 2006 Acute regulation of murine follicle-stimulating hormone β-subunit transcription by activin A. J Mol Endocrinol 36:201–220
33. Ogawa T, Yogo K, Ishida N, Takeya T 2003 Synergistic effects of activin and FSH on hyperphosphorylation of Rb and G1/S transition in rat primary granulosa cells. Mol Cell Endocrinol 210:31–38
34. Kretschmer A, Moepert K, Dames S, Sternberger M, Kaufmann J, Klippel A 2003 Differential regulation of TGF-β signaling through Smad2, Smad3 and Smad4. Oncogene 22:6748–6763
35. Piek E, Ju WJ, Heyer J, Escalante-Alcalde D, Stewart CL, Weinstein M, Deng C, Kucherlapati R, Bottinger EP, Roberts AB 2001 Functional characterization of transforming growth factor β signaling in Smad2- and Smad3-deficient fibroblasts. J Biol Chem 276:19945–19953
36. Tomic D, Miller KP, Kenny HA, Woodruff TK, Hoyer P, Flaws JA 2004 Ovarian follicle development requires Smad3. Mol Endocrinol 18:2224–2240
37. Suszko MI, Balkin DM, Chen Y, Woodruff TK 2005 Smad3 mediates activin-induced transcription of follicle-stimulating hormone β-subunit gene. Mol Endocrinol 19: 1849–1858

38. Sicinski P, Donaher JL, Geng Y, Parker SB, Gardner H, Park MY, Robker RL, Richards JS, McGinnis LK, Biggers JD, Eppig JJ, Bronson RT, Elledge SJ, Weinberg RA 1996 Cyclin D2 is an FSH-responsive gene involved in gonadal cell proliferation and oncogenesis. Nature 384: 470–474
39. Cook RW, Thompson TB, Jardetzky TS, Woodruff TK 2004 Molecular biology of inhibin action. Semin Reprod Med 22:269–276
40. Vale W, Wiater E, Gray P, Harrison C, Bilezikjian L, Choe S 2004 Activins and inhibins and their signaling. Ann NY Acad Sci 1038:142–147
41. Vale W, Rivier J, Vaughan J, McClintock R, Corrigan A, Woo W, Karr D, Spiess J 1986 Purification and characterization of an FSH releasing protein from porcine ovarian follicular fluid. Nature 321:776–779
42. Gray PC, Greenwald J, Blount AL, Kunitake KS, Donaldson CJ, Choe S, Vale W 2000 Identification of a binding site on the type II activin receptor for activin and inhibin. J Biol Chem 275:3206–3212
43. Looyenga BD, Hammer GD 2006 Origin and identity of adrenocortical tumors in inhibin knockout mice: implications for cellular plasticity in the adrenal cortex. Mol Endocrinol 20:2848–2863
44. Matzuk MM, Finegold MJ, Mather JP, Krummen L, Lu H, Bradley A 1994 Development of cancer cachexia-like syndrome and adrenal tumors in inhibin-deficient mice. Proc Natl Acad Sci USA 91:8817–8821
45. Matzuk MM, Finegold MJ, Su JG, Hsueh AJ, Bradley A 1992 α-Inhibin is a tumour-suppressor gene with gonadal specificity in mice. Nature 360:313–319
46. Kumar TR, Wang Y, Matzuk MM 1996 Gonadotropins are essential modifier factors for gonadal tumor development in inhibin-deficient mice. Endocrinology 137: 4210–4216
47. Shikone T, Matzuk MM, Perlas E, Finegold MJ, Lewis KA, Vale W, Bradley A, Hsueh AJ 1994 Characterization of gonadal sex cord-stromal tumor cell lines from inhibin-α and p53-deficient mice: the role of activin as an autocrine growth factor. Mol Endocrinol 8:983–995
48. Burns KH, Agno JE, Sicinski P, Matzuk MM 2003 Cyclin D2 and p27 are tissue-specific regulators of tumorigenesis in inhibin α knockout mice. Mol Endocrinol 17: 2053–2069
49. Kumar TR, Palapattu G, Wang P, Woodruff TK, Boime I, Byrne MC, Matzuk MM 1999 Transgenic models to study gonadotropin function: the role of follicle-stimulating hormone in gonadal growth and tumorigenesis. Mol Endocrinol 13:851–865
50. Beuschlein F, Looyenga BD, Bleasdale SE, Mutch C, Bavers DL, Parlow AF, Nilson JH, Hammer GD 2003 Activin induces x-zone apoptosis that inhibits luteinizing hormone-dependent adrenocortical tumor formation in inhibin-deficient mice. Mol Cell Biol 23:3951–3964
51. Risma KA, Clay CM, Nett TM, Wagner T, Yun J, Nilson JH 1995 Targeted overexpression of luteinizing hormone in transgenic mice leads to infertility, polycystic ovaries, and ovarian tumors. Proc Natl Acad Sci USA 92: 1322–1326
52. Zhu Y, Richardson JA, Parada LF, Graff JM 1998 Smad3 mutant mice develop metastatic colorectal cancer. Cell 94:703–714
53. Burns KH, Owens GE, Ogbonna SC, Nilson JH, Matzuk MM 2003 Expression profiling analyses of gonadotropin responses and tumor development in the absence of inhibins. Endocrinology 144:4492–4507
54. Richards JS, Sharma SC, Falender AE, Lo YH 2002 Expression of FKHR, FKHRL1, and AFX genes in the rodent ovary: evidence for regulation by IGF-I, estrogen, and the gonadotropins. Mol Endocrinol 16:580–599
55. Brown CW, Li L, Houston-Hawkins DE, Matzuk MM 2003 Activins are critical modulators of growth and survival. Mol Endocrinol 17:2404–2417
56. Matzuk MM, Kumar TR, Vassalli A, Bickenbach JR, Roop DR, Jaenisch R, Bradley A 1995 Functional analysis of activins during mammalian development. Nature 374: 354–356
57. Kadakia R, Arraztoa JA, Bondy C, Zhou J 2001 Granulosa cell proliferation is impaired in the Igf1 null ovary. Growth Horm IGF Res 11:220–224
58. Zhou J, Kumar TR, Matzuk MM, Bondy C 1997 Insulin-like growth factor I regulates gonadotropin responsiveness in the murine ovary. Mol Endocrinol 11:1924–1933
59. Liu JL, Yakar S, LeRoith D 2000 Conditional knockout of mouse insulin-like growth factor-1 gene using the Cre/loxP system. Proc Soc Exp Biol Med 223:344–351
60. Cullen KA, McCool J, Anwer MS, Webster CR 2004 Activation of cAMP-guanine exchange factor confers PKA-independent protection from hepatocyte apoptosis. Am J Physiol Gastrointest Liver Physiol 287:G334–G343
61. de Rooij J, Boenink NM, van Triest M, Cool RH, Wittinghofer A, Bos JL 1999 PDZ-GEF1, a guanine nucleotide exchange factor specific for Rap1 and Rap2. J Biol Chem 274:38125–38130
62. de Rooij J, Zwartkruis FJ, Verheijen MH, Cool RH, Nijman SM, Wittinghofer A, Bos JL 1998 Epac is a Rap1 guanine-nucleotide-exchange factor directly activated by cyclic AMP. Nature 396:474–477
63. Mei FC, Qiao J, Tsygankova OM, Meinkoth JL, Quilliam LA, Cheng X 2002 Differential signaling of cyclic AMP: opposing effects of exchange protein directly activated by cyclic AMP and cAMP-dependent protein kinase on protein kinase B activation. J Biol Chem 277: 11497–11504
64. Nechamen CA, Thomas RM, Cohen BD, Acevedo G, Poulikakos PI, Testa JR, Dias JA 2004 Human follicle-stimulating hormone (FSH) receptor interacts with the adaptor protein APPL1 in HEK 293 cells: potential involvement of the PI3-kinase pathway in FSH signaling. Biol Reprod 71:629–636
65. Miaczynska M, Christoforidis S, Giner A, Shevchenko A, Uttenweiler-Joseph S, Habermann B, Wilm M, Parton RG, Zerial M 2004 APPL proteins link Rab5 to nuclear signal transduction via an endosomal compartment. Cell 116:445–456
66. Mitsuuchi Y, Johnson SW, Sonoda G, Tanno S, Golemis EA, Testa JR 1999 Identification of a chromosome 3p14.3–21.1 gene, APPL, encoding an adaptor molecule that interacts with the oncoprotein-serine/threonine kinase AKT2. Oncogene 18:4891–4898

Molecular Endocrinology **is published monthly by The Endocrine Society (http://www.endo-society.org), the foremost professional society serving the endocrine community.**